Lower Electrical Membrane Potential and Altered pH_i Homeostasis in Multidrug-Resistant (MDR) Cells: Further Characterization of a Series of MDR Cell Lines Expressing Different Levels of P-Glycoprotein†,‡

Paul D. Roepe,* Li Yong Wei, Jonathon Cruz, and Dianne Carlson

Program in Molecular Pharmacology & Therapeutics, Memorial Sloan-Kettering Cancer Center, and Graduate School of Medical Sciences, Cornell University, 1275 York Avenue, New York, New York 10021

Received February 25, 1993; Revised Manuscript Received May 26, 1993●

ABSTRACT: Recently [Roepe, P. D. (1992) *Biochemistry 31*, 12555–12564], increased steady-state levels of chemotherapeutic drug efflux from multidrug-resistant (MDR) myeloma cells were correlated with intracellular alkalinization. To better understand elevated pH_i in MDR cells, Na^+- and Cl^--dependent recovery of pH_i upon intracellular acid or alkaline shock has been examined for this same series of MDR cell lines. In agreement with another recent report [Boscoboinik, D., Gupta, R. S., & Epand, R. M. (1990) *Br. J. Cancer 61*, 568–572], we find that the rate of Na^+-induced alkalinization after an intracellular acid shock is increased in the MDR cells, relative to the drug-sensitive parent. Interestingly, we also now find that mRNA encoding the human Na^+/H^+ exchanger (NHE) is overexpressed in these MDR cells, but the level of overexpression does not correlate with the relative drug resistance or steady-state pH_i. It is also found that the efficiency of Cl^--dependent reacidification of pH_i after an intracellular alkaline shock is reduced in the MDR cells. This effect appears to correlate with the relative expression of MDR protein, but not the relative expression of Cl^-/HCO_3^- exchanger (AE), which we now find is also altered in the series of cells. Since elevated pH_i will increase ΔpH across the plasma membrane, we have also measured the electrical potential for these cells using three different methods. Most interestingly, the magnitude of the plasma membrane electrical potential ($\Delta\Psi$) decreases concomitant with increased expression of the MDR protein. Energy provided by increased ΔpH compensates for the lowered $\Delta\Psi$, such that the total electrochemical membrane potential ($\Delta\mu_{H^+}$) remains similar among the cells in this series ($\Delta\mu_{H^+} = \Delta\Psi - Z\Delta pH$). These data, along with other recent experiments that associated an increased Cl^- conductance with the expression of MDR protein [Valverde, M., Diaz, M., Sepúlveda, F. V., Gill, D. R., Hyde, S. C., & Higgins, C. F. (1992) *Nature 355*, 830–833], are consistent with a model for MDR protein-mediated multidrug resistance that does not entail direct active transport of lipophilic drugs by the MDR protein.

Upon continued exposure to a single chemotherapeutic (*e.g.*, the anthracycline doxorubicin), many tumor cells develop multidrug resistance (MDR),[1] that is, they become cross-resistant to other chemotherapeutics (*e.g.*, the antimitotics vinblastine and colchicine) during selection, while they become resistant to the selecting agent (Biedler & Rheim, 1970). In addition, many MDR cells exhibit significant resistance to non-chemotherapeutic compounds such as gramicidin D and Tween 80. MDR is often, but not always [*cf.* Cole *et al.* (1992)], associated with increased expression of the MDR protein or P-glycoprotein (Endicott & Ling, 1989) and decreased retention of the chemotherapeutics (Gottesman & Pastan, 1988; Hammond *et al.*, 1989).

A model for MDR consistent with some data, including observed photolabeling of the MDR protein (Cornwell *et al.*, 1986; Safa, 1988), has been proposed wherein the MDR protein catalyzes the active, outward-directed transport of a variety of chemotherapeutics including anthracyclines, vinca alkaloids, and colchicine [*i.e.*, the protein performs multisubstrate active efflux; *cf.* Gottesman and Pastan (1988) and Higgins and Gottesman (1992)]. However, direct support for this model *via* the observation of either active transport of any drug against a significant concentration gradient or rate enhancement in the drug efflux process due exclusively to MDR protein and not to volume or various $\Delta\mu_{H^+}$ perturbations has not yet been unequivocally obtained.

An alternative or perhaps complementary [see Gill *et al.* (1992)] explanation for MDR is based on recent observations of increased intracellular pH (pH_i) in MDR cells (Keizer & Joenje, 1989; Boscoboinik *et al.*, 1990; Thiebaut *et al.*, 1990; Roepe, 1992; P. D. Roepe, S. Basu, and D. Carlson, unpublished data; I. Luz, P. Gros, and P. D. Roepe, unpublished data) and on the fact that the chemotherapeutic

† This research was performed in the Sackler Laboratory of Membrane Biophysics at the Sloan-Kettering Institute and was supported by grants from the Raymond & Beverly Sackler Foundation, the Society of Sloan-Kettering, and a Cancer Center Support Grant (No. NCI-P30-CA-08748). P.D.R. is a Sackler Scholar at MSKCC.

‡ A preliminary account of this work was presented at the 46th Annual Meeting of the Society of General Physiologists, September 10–13, 1992, Woods Hole, MA [Roepe, P. D., Carlson, D., Scott, H., & Wei, L.-Y. (1992) *J. Gen. Physiol. 100*, 52a].

* Author to whom correspondence should be addressed at the Memorial Sloan-Kettering Cancer Center.

● Abstract published in *Advance ACS Abstracts,* September 15, 1993.

[1] Abbreviations: MDR, multidrug resistance; pH_i, intracellular pH; NHE, Na^+/H^+ exchanger; AE, Cl^-/HCO_3^- exchanger, ΔpH, pH gradient across the plasma membrane; $\Delta\Psi$, plasma membrane electrical potential; $\Delta\mu_{H^+}$, electrochemical plasma membrane potential; $diSC_3(5)$, 3,3′-dipropylthiadicarbocyanine iodide; bis-oxonol, bis(1,3-diethylthiobarbituric acid)trimethine oxonol; di-4-ANEPPS, (dialkylamino)naphthalene pyridinium styryl; BCECF, 2′,7′-bis(carboxyethyl)-5,6-carboxyfluorescein; SNARF, carboxyseminaphthorhodafluor-1; SITS, 4-acetamido-4′-(isothiocyanato)stilbene-2,2′-disulfonic acid; EDTA, ethylenediaminetetraacetic acid; SDS, sodium dodecyl sulfate; 1× SSC, 150 mM sodium chloride/15 mM sodium citrate; HEPES, *N*-(2-hydroxyethyl)piperazine-*N*′-(2-ethanesulfonic acid); BSA, bovine serum albumin; pH_o, external pH; HBSS, Hank's balanced salt solution; β_i, intrinsic buffering capacity; rPO, acidic ribosomal phosphoprotein PO; $Z = 2.3RT/F$, where R and F are the gas and Faraday constants, respectively, and T is temperature.

0006-2960/93/0432-11042$04.00/0

drugs to which MDR cells are resistant are hydrophobic weak bases and/or that they react with their intracellular targets in a highly pH-dependent manner (*e.g.*, colchicine *vs* monomeric tubulin). Thus, elevated pH_i is expected to lead to lowered charge-dependent cytoplasmic sequestration of these compounds and/or lower efficiency of drug binding to DNA, tubulin, or other targets by "titrating out" pharmacologically relevant drug and/or pertinent binding sites [*cf.* Beck *et al.* (1983), Siegfried *et al.* (1985), and Roepe (1992)]. In addition, most of the compounds to which MDR cells are resistant are lipophilic cations at physiological pH; thus, the relative magnitude of plasma membrane electrical potential ($\Delta\Psi$) will affect their intracellular partitioning. Since ΔpH is only one component of total electrochemical membrane potential ($\Delta\mu_{H^+} = \Delta\Psi + \Delta pH$), elevated pH_i at constant pH_o might be expected to alter $\Delta\Psi$ (or vice versa). Thus, a corollary of this theory is that changes in pH_i for MDR cells might reflect changes in $\Delta\Psi$ which could further contribute to altering the level of retained chemotherapeutic (Roepe *et al.*, 1992).

In support of this idea, it has recently been reported that increased pH_i is correlated with increased resistance to the weakly basic lipophile, doxorubicin (Kiezer & Joenje, 1989; Roepe, 1992), which is also conspicuously cationic. Moreover, the steady-state level of doxorubicin efflux (but *not* the initial rate) has been shown to be qualitatively related to increased MDR protein expression in a series of MDR cells expressing varied amounts of MDR protein but *linearly* related to pH_i (Roepe, 1992). In addition, Higgins, Sepúlveda, and colleagues have recently demonstrated that MDR protein may mediate Cl^- translocation across the plasma membrane (Valverde *et al.*, 1992; Gill *et al.*, 1992). Since Cl^- is crucial for the regulation of pH_i, intracellular volume, and membrane potential, it is conceivable that this activity of MDR protein potentially alters pH_i homeostasis.

Thus, we have investigated how MDR cells maintain an elevated pH_i in order to better understand any role that MDR protein might play in these phenomena. Since the MDR phenotype is complicated, our approach to elucidating the contribution of MDR protein involves studying *trends* in *series* of cells expressing varied amounts of MDR protein. If the extent of an observed phenotypic alteration correlates with relative MDR protein expression, we tentatively attribute it to some aspect of MDR protein function.

In this report, we show that upon an intracellular acid shock MDR cells exhibit increased Na^+/H^+ antiport activity, relative to the sensitive parent, and that pretreatment with the chemosensitizer verapamil partially abrogates increased Na^+/H^+ exchange. Interestingly, the relative rate of Na^+/H^+ antiport appears to correlate with the relative expression of Na^+/H^+ antiporter as assayed by Northern blot; however, steady-state pH_i does not. In addition, drug-sensitive 8226 cells are observed to reacidify after an intracellular alkaline shock in the absence of Cl^- upon subsequent addition of Cl^-, but recovery for MDR cells expressing significant MDR protein is impaired. This defect appears to be related to the expression of MDR protein, but not the relative expression of anion exchangers, which are also found to be altered in the series of MDR cell lines.

Along with elevated pH_i and altered expression of antiporters involved in pH_i homeostasis, these cells exhibit decreased electrical membrane potential ($\Delta\Psi$) as evidenced by fluorescence measurements with the voltage-sensitive dyes $diSC_3$-(5), bis-oxonol, and di-4-ANEPPS. The relative millivolt decrease in $\Delta\Psi$ appears to be related to the relative expression of MDR protein in the series of 8226-derived cells, and it parallels the calculated millivolt *increase* in ΔpH for the series (Roepe, 1992). These data in their entirety suggest that, for some cells, the molecular-level consequence of MDR protein overexpression includes the near-stoichiometric "exchange" of energy stored as $\Delta\Psi$ into energy stored as ΔpH, such that $\Delta\mu_{H^+}$ remains relatively constant.

Although more detailed experiments with vesicles and proteoliposomes will be required to fully define the ion transport alterations that cause these phenomena, these data, along with other recent reports (Valverde *et al.*, 1992; Gill *et al.*, 1993), are consistent with an alternative model for MDR protein-mediated MDR. It is suggested that the ion translocating ability of MDR protein disrupts normal pH_i homeostasis and electrical membrane potential without severely impairing $\Delta\mu_{H^+}$. Both lowered $\Delta\Psi$ and increased pH_i are expected to confer broad cellular resistance to lipophilic cations and hydrophobic weak bases, respectively, and/or hydrophobic compounds that bind to cellular targets in a highly pH_i-dependent manner. Along with other recent data that show there is no rate enhancement in chemotherapeutic drug efflux for these cells (Roepe, 1992), these data argue that MDR protein indirectly mediates decreased drug retention without performing active drug transport.

MATERIALS AND METHODS

Materials. 3,3′-Dipropylthiadicarbocyanine iodide ($diSC_3$-(5)), bis(1,3-diethylthiobarbituric acid)trimethine oxonol (bis-oxonol), 2′,7′-bis(carboxyethyl)-5,6-carboxyfluorescein (BCECF), carboxyseminaphthorhodafluor-1 (SNARF), nigeicin, valinomycin, and the (dialkylamino)naphthalene pyridinium styryl dye (di-4-ANEPPS) were purchased from Molecular Probes (Eugene, OR) and used without further purification. 4-Acetamido-4′-(isothiocyanato)stilbene-2,2′-disulfonic acid (SITS) and amiloride were from Sigma. [^{14}C]-Inulin and ^3H_2O were from New England Nuclear; the high molecular weight fraction of inulin was purified before use by passage over a Sephadex G-50 column. All other chemicals were reagent grade or better, purchased from commercial sources, and used without further purification.

Tissue Culture. The drug-sensitive myeloma cell line RPMI 8226 and the drug-resistant lines Dox 1, Dox 6, and Dox 40 were the kind gift of Dr. William S. Dalton (University of Arizona Cancer Center) and were cultured as described (Dalton *et al.*, 1989; Roepe, 1992). The Dox 120 cell line was raised by single-step selection of the Dox 40 line in 1.2×10^{-6} M doxorubicin. These cells are significantly cross-resistant to vincristine and other chemotherapeutics and have been shown to significantly overexpress MDR protein as well as exhibit increased steady-state levels of doxorubicin efflux (Dalton *et al.*, 1989; Roepe, 1992).

Isolation of mRNA and Northern Blot Analysis. Total cellular RNA was isolated by the method of Chomczynski *et al.* (1987). Poly(A^+)RNA was selected by passing total RNA dissolved in 0.5 M NaCl/20 mM Tris/1 mM EDTA/0.1% Sarcosyl (pH 7.6) through an oligo(dT)–cellulose column and eluting with 10 mM Tris/1 mM EDTA/0.05% SDS (pH 7.6) as described (Sambrook *et al.*, 1989).

Poly(A^+)RNA (5 μg) was denatured with formaldehyde, size-fractionated by 1.2% agarose gel electrophoresis, and subsequently transferred to a nylon membrane filter (Schleicher & Schuell, Keene NH) by capillary blotting. Membranes were prehybridized in 6× SSC/2X Denhardts/0.1% SDS for 4 h at 68 °C and hybridized at the same temperature overnight with labeled probe in 6× SSC/0.5% SDS/100 μg/mL denatured salmon sperm DNA. Probes were labeled

by the random priming method and purified by passage through a Sephadex G-50 spin column before use. Blots were washed once at room temperature in 2× SSC for 20 min, twice at 68 °C in 0.2× SSC/0.5% SDS for 30 min, and then 2–3 times more at 68 °C in 0.1× SSC/0.5% SDS for 30 min before imaging radioactivity. Blots probed more than once were stripped by washing at 88 °C in 0.1X SSC/0.5% SDS for 3 h. Bands were visualized either by autoradiography (we used Kodak X-OMAT AR film; exposure times varied between 4 and 48 h, see captions) or by imaging β-radiation with a betascope 603 blot analyzer (Betagen). For quantitative imaging, the bands of interest were first normalized relative to background emission detected by the betascope. To calculate relative levels of NHE, AE, or MDR mRNA, the signal from a given mRNA preparation was normalized relative to the signals for β-actin and acidic ribosomal phosphoprotein PO (rPO) (see Results). The ratio of β-actin/rPO band intensities was the same for each cell line, in multiple mRNA preparations and multiple Northern blots.

Fluorescence Spectroscopy. Fluorescence spectra were obtained with a Photon Technologies Inc. (New Brunswick, NJ) fluorometer interfaced to an AST Research personal computer. Sample cuvettes were jacketed within an aluminum holder, and the temperature was controlled by a circulating water bath. In most cases, cell suspensions were rapidly mixed with a magnetic stirrer situated beneath the cuvette. Excitation/emission wavelengths and the other parameters of various experiments may be found in the individual figure captions.

Na^+/H^+ Exchange and Cl^--Dependent Reacidification. To monitor changes in intracellular pH (pH_i) upon intracellular acidification or alkalinization, cells were harvested by centrifugation for 10 min at 1000 rpm in a Sorval RT6000B centrifuge and resuspended in HEPES or HCO_3^--buffered balanced salt solutions, pH 7.30, with 10 mM glucose. They were then passively loaded with the acetoxymethyl form of BCECF (BCECF-AM) (2.5 μM, final concentration) for 30 min at 37 °C. The acetoxymethyl form is trapped within the cytoplasm upon diffusion into the cell and subsequent cleavage by cytoplasmic esterases, which introduces a –4 charge to the compound. Cells were washed in balanced salts with glucose to remove uninternalized dye before spectra were obtained, and in general were rapidly diluted into a 3-mL cuvette while spectra were being obtained in a darkened room. In some experiments, cells were also successfully loaded with dye in the presence of RPMI culture medium with additional 10% fetal calf serum, washed with balanced salts, and diluted into balanced salts ± HCO_3^-. Buffers harboring HCO_3^- were equilibrated with CO_2 and continuously purged to ensure stable pH, which was verified with a reference microelectrode (Microelectrodes, Inc., Londonderry, NH).

To acid or alkaline shock cells, nigericin (0.33–0.66 μM) was added to suspensions of 1×10^6 cells in either Na^+-free acidifying buffer (105 mM choline chloride/40 mM KCl/10 mM HEPES/2 mM $CaCl_2$/1 mM $MgCl_2$, pH 6.6–6.9) or Cl^--free alkalinizing buffer (105 mM sodium glutamate/40 mM potassium glutamate/10 mM HEPES/2 mM $CaSO_4$/1 mM $MgSO_4$, pH 8.0), respectively, and intracellular acidification or alkalinization was stopped by the addition of bovine serum albumin (BSA) to 5 mg/mL, as previously described in detail by Grinstein and colleagues (Grinstein *et al.*, 1984). Alternatively, transient acidification was induced by preincubation with 15 mM NH_4Cl and dilution into NH_3-free buffer as described by Roos and Boron (1981). Transient alkalinization by diffusion of acetate yielded somewhat irreproducible results; thus, the nigericin/BSA method was preferred for intracellular alkalinization. After clamping pH_i to a desired value, initiation of Na^+-dependent realkalinization or Cl^--dependent reacidification was by the addition of 25–50 mM Na^+- or Cl^--containing salts, respectively (see Results).

Standardization of BCECF excitation ratios or SNARF emission ratios *vs* pH_i was by the nigericin/K^+ method, with a microelectrode simultaneously monitoring external pH (pH_o) as a reference. Standard curves for resistant and sensitive cells were superimposable (data not shown), and the minuscule leak of dye that occurred during the time course of the measurements was the same for resistant and sensitive cells. Nearly linear standard curves were obtained for the pH ranges 7.1–8.0 and 6.6–7.0.

To calculate H^+ flux rates, the pH_i change per unit time (calculated from a straight-line fit of the first 45 s of the pH_i recovery curve; see Results) was multiplied by the value of the intrinsic buffering capacity (β_i; see below) measured for the particular cell at the pH_i at which recovery was initiated. Additional details may be found in the appropriate figure or table captions.

Determination of Intracellular Buffering Capacity. Buffering capacity was determined in the absence of bicarbonate by monitoring pH_i alterations upon diffusion of the weak base ammonium as described in detail elsewhere (Roos & Boron, 1981). Cells were loaded with BCECF as described above, and their pH_i values were clamped by the Grinstein method (Grinstein *et al.*, 1984) as described above. pH_i was constantly monitored by ratioing 439- and 505-nm excitation using software written by Photon Technologies Inc. (New Brunswick, NJ). When a desired pH_i was attained, NH_4Cl (2–10 mM) was added and the resultant jump in pH_i was measured (n = 3, SE (standard error) <10%). By knowing $[NH_3]_o$, assuming $[NH_3]_o = [NH_3]_i$, and using a pK_B for ammonium of 9.21, $[NH_4^+]_i$ was calculated using the Henderson–Hasselbach relation [see Roos and Boron (1981)]. Buffering capacity (β_i) was then calculated ($\beta_i = \Delta[NH_4^+]_i/\Delta[pH_i]$) for each of the cell lines clamped at seven different pH_i values between 6.6 and 8.0 (see Results). β_i *vs* pH_i curves were well fit by quadratic equations and differed slightly for the different cell lines (not shown); these data will be presented in detail elsewhere but, for example, β_i for 8226 was found to be 45, 31, and 80 mM/pH_i at pH_i 6.60, 6.90, and 7.90 respectively.

Measurement of Electrical Membrane Potential ($\Delta\Psi$). As explained in Results, we initially chose to use the fast-response styryl dye di-4-ANEPPS (Montana *et al.*, 1989; Loew *et al.*, 1993) to assess $\Delta\Psi$ due to the fact that it is very well localized to the plasma membranes of the cells used in this study (at least within the time used to make our measurements) as witnessed by fluorescence microscopy (P. D. Roepe, unpublished data) and due to the fact that the measured *ratio* of excitation at 440 and 505 nm when monitoring emission at 610 nm is dependent upon the magnitude of $\Delta\Psi$. Thus, contributions to the measured $\Delta\Psi$ from mitochondria and other organelles as well as variability in the concentration of cell-associated dye or number of cells are less of a concern, respectively. Since some investigators have suggested that hydrophobic dyes could conceivably be actively transported by the MDR protein, the latter is of considerable importance. Although di-4-ANEPPS exhibits voltage-dependent changes that are much smaller than those typically seen for oxonol and carbocyanine dyes, we felt that these benefits perhaps outweighed the disadvantages.

Nonetheless, we also performed $\Delta\Psi$ measurements with the anionic bis-oxonol and cationic carbocyanine diSC_3(5)

Table I [a]

cell line	fold resistance	relative MDR 1 protein	mean cell diameter (μm)	estimated intracellular water (μL/1 × 10^6 cells)	$[K^+]_i$ (mM)	pH_i
8226	1	ud	12.98	0.64	166	7.12
Dox 1	3	1	12.82	0.68	161	7.29
Dox 6	10	9	11.35	0.53	182	7.41
Dox 40	60	50	12.53	0.69	157	7.55
Dox 120	125	55	12.50	0.72	152	7.62

[a] Characteristics of the members of the 8226-derived series of MDR cell lines [see Dalton *et al.* (1989)]. Note that Dox 1 was derived from 8226, Dox 6 from Dox 1, Dox 40 from Dox 6, and Dox 120 from Dox 40 by increasing the concentration of doxorubicin in the growth medium. Fold resistance is relative to doxorubicin. Relative MDR protein was determined as described (Dalton *et al.*, 1986, 1989; Roepe, 1992); ud denotes undetectable. Mean particle size was determined with Coulter counter parameters (values shown are ±1.3 μm). Cell-associated K^+ was determined by flame photometry (n = 4, SE ≤7%), and $[K^+]_i$ was calculated using estimated water V_i. pH_i was determined by SNARF and/or BCECF fluroescence (SE <1.5%; values shown are the average of at least six separate determinations; Roepe, 1992). See Materials and Methods for additional details.

probes essentially as described previously (Rink *et al.*, 1980; Laris & Hoffman, 1986). Although *quantitation* of $\Delta\Psi$ by the use of bis-oxonol is typically ambiguous due to interaction with valinomycin and other hydrophobic molecules, the probe is useful in terms of qualitative descriptions of potential as well as in assessing changes in $\Delta\Psi$ upon various perturbations, and interpretation benefits from the fact that this dye is *excluded* from cells in a $\Delta\Psi$-dependent manner (see Results). Estimation of $\Delta\Psi$ with $diSC_3(5)$ has been found to be consistent with electrophysiological methods on several occasions, although some ambiguity results with the use of different dye concentrations (Rink *et al.*, 1980); thus, we used low (50 nM) concentrations of this dye in our experiments. Although the absolute magnitude of measured $\Delta\Psi$ differed for some cells upon use of the different probes, relative differences among members of the series of MDR cells expressing variable MDR protein were consistent (see Results).

$\Delta\Psi$ was calibrated by the null point K^+/valinomycin titration method of Laris and Hoffman (1986) with HBSS containing 10 mM HEPES, pH 7.30, used as the standard solution and increased $[K^+]_o$ substituting for decreased $[Na^+]_o$. Solutions harboring various $[K^+]$ and 0.5 μM di-4-ANEPPS were rapidly mixed with 5 × 10^5 cells. Rapid uptake of di-4-ANEPPS into the plasma membrane was monitored, and after a flat base line was observed 60 s later, valinomycin was added to a final concentration of 10 μM. The relative change in the ratio of 440- to 505-nm excitation (610-nm emission) was plotted as a function of external $[K^+]$ and the minimum (null point) was determined graphically (see Results). For $diSC_3(5)$ measurements, 50 nM dye (1.5 μL of a 100 μM solution in DMSO) was mixed with 3 mL of HBSS harboring various $[K^+]$ until a flat base line was achieved (Rink *et al.*, 1980). Cells (5 × 10^5) previously washed in HBSS were then added and the suspension was rapidly mixed. After equilibrium was attained (3–5 min), valinomycin was added to a final concentration of 10 μM (1.5 μL of a 20 mM solution in EtOH), and the suspension was rapidly mixed again. The change in 670-nm fluorescence (640-nm excitation) observed after the addition of ionophore was plotted *vs* external $[K^+]$, and the null point was determined graphically. Slight deviations from zero slope in the curve before the addition of ionophore were corrected by curve fitting and accounted for when plotting the data.

Qualitative characterization of electrical potential with bis-oxonol was performed by mixing cells with 100 nM dye essentially as performed with $diSC_3(5)$. Excitation was at 535 nm, and emission was monitored at 559 nm.

Measurement of $[K^+]_i$. Since measurement of $\Delta\Psi$ by the valinomycin/null point method requires knowledge of the intracellular concentration of K^+ ($[K^+]_i$), we measured cell-associated K^+ for the cell lines by flame photometry as described previously (Iversen, 1976). After intracellular volume was determined (see below), $[K^+]_i$ was calculated. Cells (2 × 10^7) were harvested and washed in 145 mM choline chloride/10 mM Tris (pH 7.3), and the pellet was dried overnight at 80 °C in an oven. The pellet was then extracted with 200 μL of 0.5 N HNO_3 for 24 h, and K^+ in the extract was measured with an Instrumentation Laboratories Model 943 flame photometer that had been calibrated with standard $[K^+]$ solutions.

Measurement of Intracellular Volume (V_i). Total cell volume was calculated after the mean particle size of cell suspensions was determined by the single threshold Coulter method (Kachel, 1990) performed with a ZM Coulter counter (Coulter Scientific Instruments, Hialeah, FL). Size/voltage calibration of the counter was with polystyrene beads (Flow Cytometry Standards Corporation, Research Triangle Park, NC) of various size. The calibration routine used allows extremely reproducible determination of particle size distributions (±0.5 μm) and thus graphical estimation of the mean particle size of a suspension of cells [see Kachel, (1990)]. The inflection points from plots of counts (n = 3, SE < 1%) *vs* voltage for polystyrene standards were used to generate a linear standard curve, which was then used to determine mean particle size from counts *vs.* voltage plots for (3–4) × 10^4 cells/mL suspensions.

Intracellular water volume was determined by ratioing [^{14}C]-inulin *vs* ^3H_2O dpm as described (Rottenberg, 1979). Cells (1 × 10^6) in 1 mL of HBSS/10 mM HEPES (pH 7.3) were incubated with 1 μCi of ^3H_2O water and 15 μCi of [^{14}C]inulin at 37 °C, and the cells were then isolated by centrifugation. Radioactivity in the supernatant and the cell pellet was quantitated with a dual-channel $^{14}C/^3H$ dpm program using a Beckman LS 5801 scintillation counter. ^{14}C and ^{3}H quench curves were also calculated using known dpm in the same buffer and scintillation fluid volumes that were used in individual experiments, and the auto quench correcting capabilities of the LS 5801 were used to maximize counting efficiency yet decrease spillover to the different channels.

RESULTS

We have adapted established techniques to study pH_i regulation in a series of MDR cells that exhibit various degrees of MDR protein expression and elevated pH_i (*cf.* Table I). Figure 1 illustrates our pH_i clamping technique, previously used to successfully assay Na^+/H^+ exchange in mass populations of other nonadherent cells [*e.g*, lymphocytes; see Grinstein *et al.* (1984) and Grinstein and Dixon (1989)]. RMPI 8226 myeloma cells were harvested as described, passively loaded with BCECF, and washed. They were then fast diluted into isotonic medium at pH 6.8 containing 40

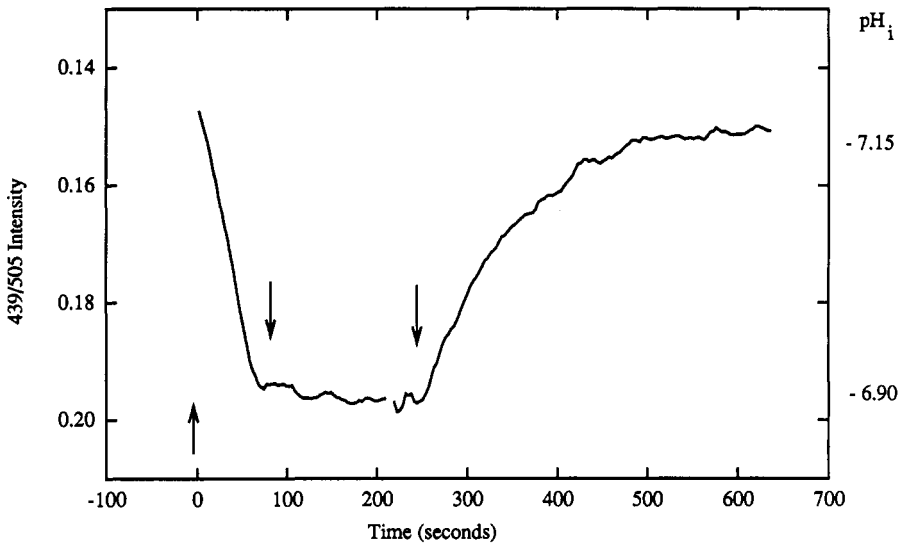

FIGURE 1: Representation of the pH_i clamping technique used in this study. As described, cells were loaded with BCECF and diluted into Na^+-free medium containing 0.66 μM nigericin to lower pH_i (first arrow). Cell viability is not affected at this concentration of nigericin [P. D. Roepe and D. Carlson, unpublished results; see also Grinstein *et al.* (1984)]. Cells were pH_i clamped by the addition of BSA to 5 mg/mL (second arrow) and reacidified by the addition of 50 mM NaCl (third arrow; similar results are obtained at lower [NaCl], but the rate of recovery is slower). The leak of BCECF during the measurement of Na^+/H^+ exchange is minuscule and is not measurably different for resistant and sensitive cells. Spectra were smoothed by the Savitzky–Golay algorithm (Savitzky & Golay, 1964) using a 15-point buffer and plotted with Sigmaplot software (Jandel Scientific, Corte Madera, CA).

mM K^+ and 0.66 μM nigericin (Figure 1, first arrow). This results in transient lowering of pH_i (*i.e.*, an increase in the ratio of 439/505-nm BCECF excitation). After a desired pH_i is attained, bovine serum albumin (BSA) is added to a final concentration of 5 mg/mL (second arrow). This halts the H^+ translocation catalyzed by nigericin. Since these cells were diluted into isotonic medium that does not contain Na^+, they cannot realkalinize *via* the Na^+/H^+ exchanger. They are therefore "clamped" to a desired pH_i that remains relatively stable in the absence of Na^+, as witnessed by the flat region of the curve from 80 to 280 s. Upon addition of Na^+ (third arrow), pH_i rapidly returns to near the resting pH_i value of these cells. An analogous experiment can be performed with these cells to transiently induce higher pH_i and a return to lower pH_i by dilution into Cl^--free buffer at high pH (~8.0) and subsequent addition of Cl^- (see below).

Increased Na^+/H^+ Exchange in MDR Cells. When sensitive 8226 or resistant Dox 6 myeloma cells are acidified as described above, rapid realkalinization is observed for both cells upon the addition of 50 mM NaCl (Figure 2). Similar data are obtained using the NH_3–pulse method (Roos & Boron, 1981; data not shown). At $pH_o = pH_i = 6.60$, realkalinization is faster for the drug-resistant cells (see also Table II). Furthermore, the MDR cells equilibrate to a higher steady-state pH_i, as previously determined in separate experiments with the pH_i indicator SNARF[2] (Roepe, 1992). Recovery is Na^+ dependent and not significantly affected by the induced change in osmotic strength, as evidenced by control experiments with 50 mM choline chloride and choline chloride/NaCl or KCl/NaCl mixtures[3] (not shown).

Figure 3 illustrates that recovery is significantly affected by the addition of amiloride along with BSA. Inhibition for the sensitive cells is about 50% at 5 μM amiloride and >90% at 100 μM, which is similar to the NHE inhibition previously observed (Grinstein *et al.*, 1984) in similar experiments with mouse lymphocytes. These initial data therefore suggest that the human myeloma cells harbor a Na^+/H^+ exchanger that exhibits "typical" amiloride sensitivity.

The results in Figure 2 are somewhat similar to data recently obtained with CH^RC5 cells, a 200-fold MDR cell line selected on colchicine (Boscoboinik *et al.*, 1990). Thus, increased NHE activity might, naively, be expected to be one way in which MDR cells maintain an elevated pH_i, although an increase in the rate of exchange as measured in a transient assay may not necessarily translate into altered $[H^+]_i$ under steady-state conditions. Furthermore, addition of amiloride to cell suspensions at pH_o 7.3 reveals that the resting activity of the antiporter is similar for the different cell lines (not shown, see Discussion). In any case, to examine this phenomenon more closely, we measured Na^+-induced alkalinization at different pH_i values for the entire series of MDR cell lines that exhibit increased MDR concomitant with increased MDR protein expression.

As shown in Table II, the rate of Na^+-induced alkalinization is altered as cells exhibit higher levels of MDR; however, the most dramatic increase in rate is for the Dox 6 line, which is only 10-fold resistant to doxorubicin and which expresses about 9-fold more MDR protein relative to the Dox 1 line (*cf.* Table

[2] Although the resistant cells do not equilibrate to exactly normal steady-state pH_i as measured in the absence of nigericin (Roepe, 1992), the small discrepancy is likely due to the rigors of these experimental conditions. The percent difference between true equilibrium pH_i *vs* the pH_i attained in these transient assays is very similar for all cell lines.

[3] Since the 8226-derived series of MDR cells does not grow as adherent monolayers, it proves difficult to alter the ionic composition of the medium on a time scale appropriate for these measurements *via* continuous perfusion or rapid change of the extracellular medium. Thus, to provide the Na^+ necessary for initiation of Na^+/H^+ exchange, salt is added to a continuously mixed suspension of these cells. Although this does alter the relative osmotic strength of the medium, a series of controls wherein equivalent concentrations of K^+- or choline-containing salts, or additional K^+ or choline along with Na^+ are added reveals that the recovery from pH_i shock witnessed in these experiments is Na^+ specific and not the result of the osmotic perturbation and that the differences noted between the cell lines are not due to different responses to similar osmotic perturbation (*e.g.*, a different relative change in volume). Furthermore, by mixing Na^+ and choline chloride solutions, it can be shown that the measured rate of recovery from acid shock is Na^+ concentration dependent [nearly linearly dependent between 10 and 75 mM Na^+; P. D. Roepe, unpublished results; see also Grinstein *et al.* [(1984)] and essentially independent of the differences in osmotic perturbation caused by the addition of 25–50 mM levels of salt.

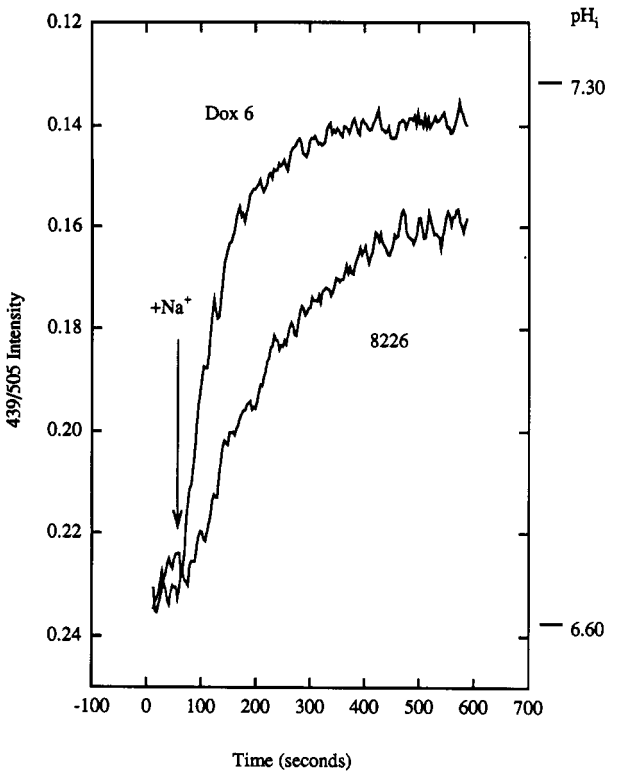

FIGURE 2: Na^+-induced alkalinization (Na^+/H^+ antiport) in drug-resistant Dox 6 (top curve) and sensitive RPMI 8226 (bottom curve) cells at pH_o 6.60. Cells were clamped to pH_i 6.60 by the nigericin/BSA method (see Materials and Methods) in a 3-mL cuvette with stirring, and 50 mM NaCl was added by rapid injection (at the arrow). The temperature was 30 °C. Note the faster rate of Na^+/H^+ antiport in the resistant cells and the higher pH_i to which the resistant cells equilibrate. Extremely slow alkalinization was observed upon the addition of BSA alone or BSA and irrelevant (K^+ or choline) salts at similar ionic strength. The presented data are representative of six separate experiments. Data are not smoothed.

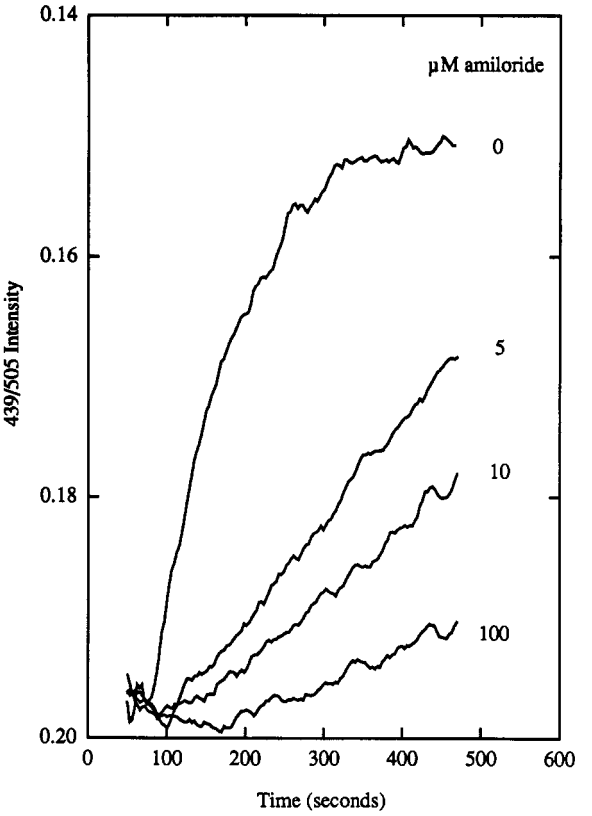

FIGURE 3: Effect of the Na^+/H^+ exchanger inhibitor amiloride on the Na^+-induced realkalinization of 8226 cells. Amiloride was added immediately before the addition of 50 mM Na^+ to a final concentration of (from top) 0, 5, 10, and 100 μM. Data are smoothed as for Figure 1.

I). Notably, the more resistant Dox 40 and Dox 120 cells exhibit a considerably slower rate of Na^+-induced alkalinization but a higher pH_i relative to Dox 6 (*cf.* Tables I and II).

To examine one possible explanation for this, we isolated mRNA and probed for expression of NHE using a 1.9-kbp (kilobase pair) *Bam*HI fragment of the human NHE 1 cDNA (Sardet *et al.*, 1989). Figure 4 shows an autoradiogram of the Northern blot, and Table II summarizes NHE expression after normalization of the signal (see Materials and Methods) to those for both β-actin and human acidic ribosomal phosphoprotein PO (rPO) (Laborda, 1991; Masiakowski *et al.*, 1982). Interestingly, the levels of mRNA encoding NHE are increased for all of the MDR cells relative to 8226, although some levels of overexpression are minor (yet consistently seen in several blots using several mRNA preparations). Overexpression is better than 10-fold for the Dox 6 line, which also conspicuously exhibits the greatest increase in the rate of Na^+-induced alkalinization (*cf.* Table II). Similarly, the increased rates of Na^+-induced alkalinization correlate qualitatively with NHE overexpression in the other members of this series. Importantly, however, as measured previously (Roepe, 1992) steady-state pH_i increases for more resistant members of the series (*cf.* Table I), even though NHE overexpression *decreases* after peaking for the Dox 6 cell line (compare Figure 4 and Table II).[4]

Interestingly, as reported previously (Boscoboinik *et al.*, 1990) simultaneous addition of 10–50 μM verapamil with 50 mM Na^+ does not significantly change the rate or extent of pH_i recovery for either cell type (not shown). However, we now find that preincubation with 10 μM verapamil for 30 min before dilution into Na^+-free medium affects Na^+/H^+ exchange for the resistant cells (Figure 5) such that they equilibrate to a pH_i 0.2–0.3 pH unit lower (*i.e.*, the set point of exchange is perhaps altered). The initial rate of alkalinization is apparently unaffected. A less dramatic effect is seen for the sensitive cells (not shown). It has also been found that verapamil lowers the steady-state pH_i and diminishes the increased steady-state level of doxorubicin efflux from these cells (Roepe, 1992; P. D. Roepe, unpublished data). A more detailed analysis of this effect for these and other MDR cell lines will be published elsewhere.

Decreased Cl^--Dependent Reacidification after Intracellular Alkaline Shock. Experiments analogous to the Na^+-induced realkalinization measurements can be performed to assay the ability to reacidify in a Cl^--dependent manner. When the cells are alkalinized by dilution into Cl^--free buffer at pH_o 8.0 in the presence of 0.66 μM nigericin and then induced to reacidify by the addition of 30 mM Cl^- (Figure 6A, Table II), differences can be seen in the rate of pH_i recovery. Independent of the pH_i reached during alkalinization, the 60- or 120-fold resistant cells reacidify slowly upon the addition of Cl^- whereas the sensitive cells recover more rapidly. Similar recovery for the 8226 cells is seen upon the addition of either

[4] We attempted to verify overexpression of NHE by immunoprecipitation of the protein with available polyclonal antisera (S. Grinstein and P. D. Roepe, unpublished data), but were unsuccessful due to poor reactivity of the available antibody with the NHE isoform present in these cells (S. Grinstein, personal communication). Nonetheless, the correlation between NHE mRNA and relative rates of Na^+-induced alkalinization (Table II) argues that increased exchanger is present in the plasma membranes of these cells.

Table II [a]

cell line	rate of Na^+-induced alkalinization (mM H^+/s)		rate of Cl^--induced acidification (mM H^+/s) at pH_i 7.75	relative fold expression of mRNA encoding		
	pH_i 6.60	pH_i 6.90		NHE	AE2	MDR
8226	4.01	2.06	35.7	1	1	ud
Dox 1	9.52	2.16	26.0	2.2	11.0	ud
Dox 6	96.1	55.8	25.0	12.6	3.0	1
Dox 40	9.41	3.11	8.22	2.2	2.2	>50
Dox 120	9.50	3.50	8.1	3.2	3.4	>50

[a] Calculated rates of Na^+-induced alkalinization and Cl^--induced acidification upon addition of 50 mM NaCl to cell suspensions transiently acidified or alkalinized in the Grinstein method (see Materials and Methods). Rates were calculated after the intracellular buffering capacity was determined for the different cells at the appropriate pH_i (see Materials and Methods; note that a β_i *vs* pH_i plot is not linear). Relative expression of the various ion transporters was determined by quantitative imaging of Northern blots with a betascope β-imager (see Materials and Methods) after correcting for background emission and scaling to β-actin and acidic ribosomal phosphoprotein PO mRNA (see Materials and Methods; the ratios of the two control mRNAs varied by <10% for the different cell lines, and thus the calculated fold overexpression is the same regardless of the control mRNA used). Values are representative of several blots using different mRNA preparations. ud denotes undetectable. See Table I for levels of MDR protein detected by immunoblot with the antibody C219; note that, although the immunoreactive protein is easily seen [*cf.* Dalton *et al.* (1989)], mRNA levels remain low in the less resistant lines.

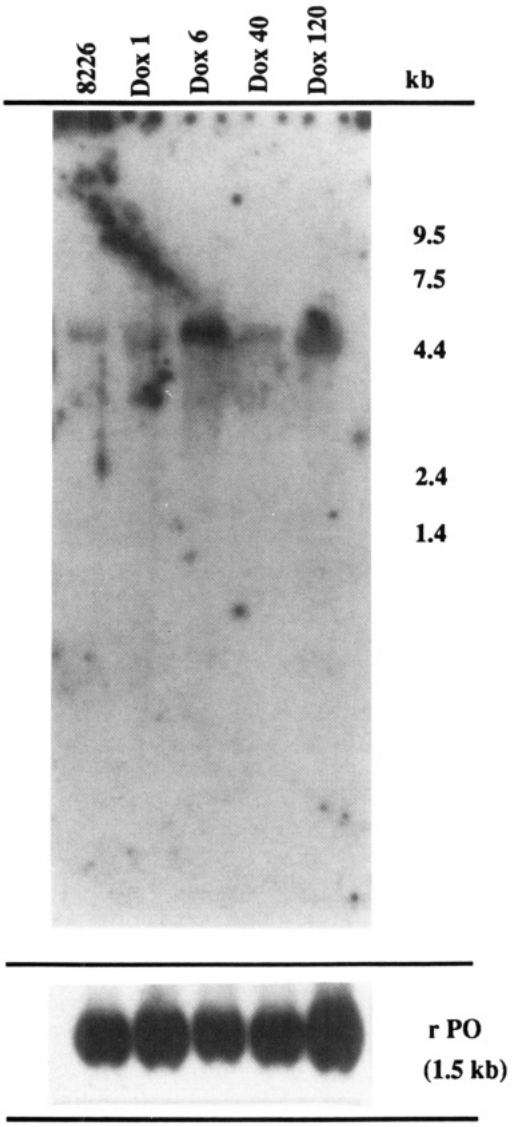

FIGURE 4: Northern blot analysis of relative NHE expression for the members of the MDR series. Purified mRNA (5 μg) was electrophoresed and transferred to nitrocellulose (see Materials and Methods) before probing with a hu NHE 1 cDNA fragment. Also shown (bottom) is the result obtained after the same blot is probed for rPO. Quantitation of the 4.9-kbp NHE band for the different mRNA preparations was as described in Materials and Methods and is summarized in Table II. Exposure times were 16 (top, NHE) and 4 h (bottom, rPO).

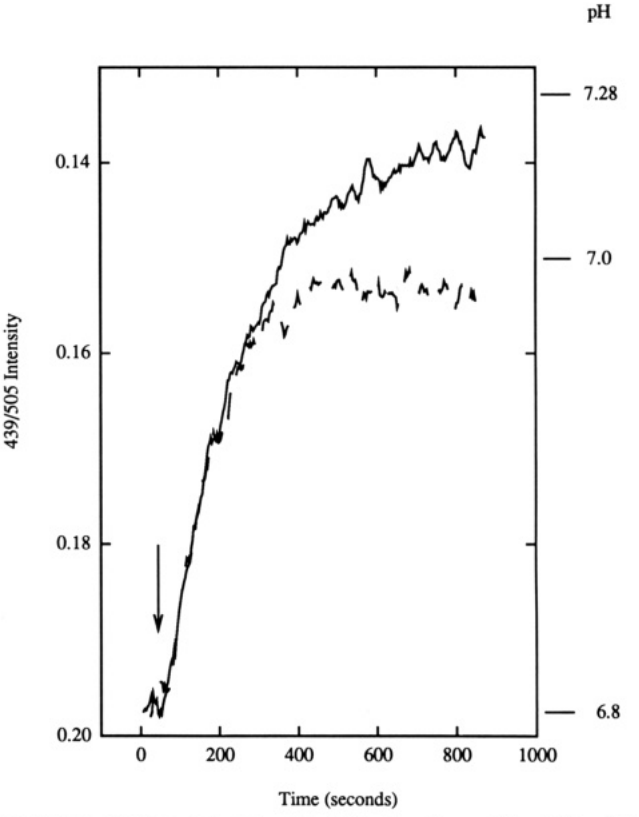

FIGURE 5: Sodium-induced realkalinization for resistant Dox 40 cells before (solid line) and after (dashed line) preincubation with 10 μM verapamil for 30 min at 37 °C. Note that the treated cells equilibrate to lower pH_i, but perform exchange at nearly the same initial rate. Similar effects are also seen after treatment with lower concentrations of verapamil for longer times, but not upon addition of verapamil with Na^+ (not shown). Data are not smoothed.

choline chloride, KCl, or NaCl and is somewhat more dependent on the osmotic perturbation than is Na^+-dependent realkalinization by this assay (see footnote 3). However, controls analogous to those described in footnote 3 reveal that recovery is not due to the osmotic perturbation *per se* and that it is Cl^- dependent.

Recovery for the sensitive cells is inhibitable by SITS (Figure 6B); thus, it is likely that reacidification is due at least in part to Cl^-/HCO_3^- exchange, as would be true for many cell types. However, the concentration of stilbene required for complete inhibition is high (≥1 mM), relative to the concentrations previously found to inhibit the Cl^-/HCO_3^- exchanger(s) found in erythrocytes ($K_i \approx 5$ μM) and HL60 cells (inhibited by 100–200 μM SITS). Notably, however, the recently isolated nonerythroid anion exchanger isoform 2 (AE2) is only blocked by about 74% upon addition of 400 μM stilbene (Lee *et al.*,

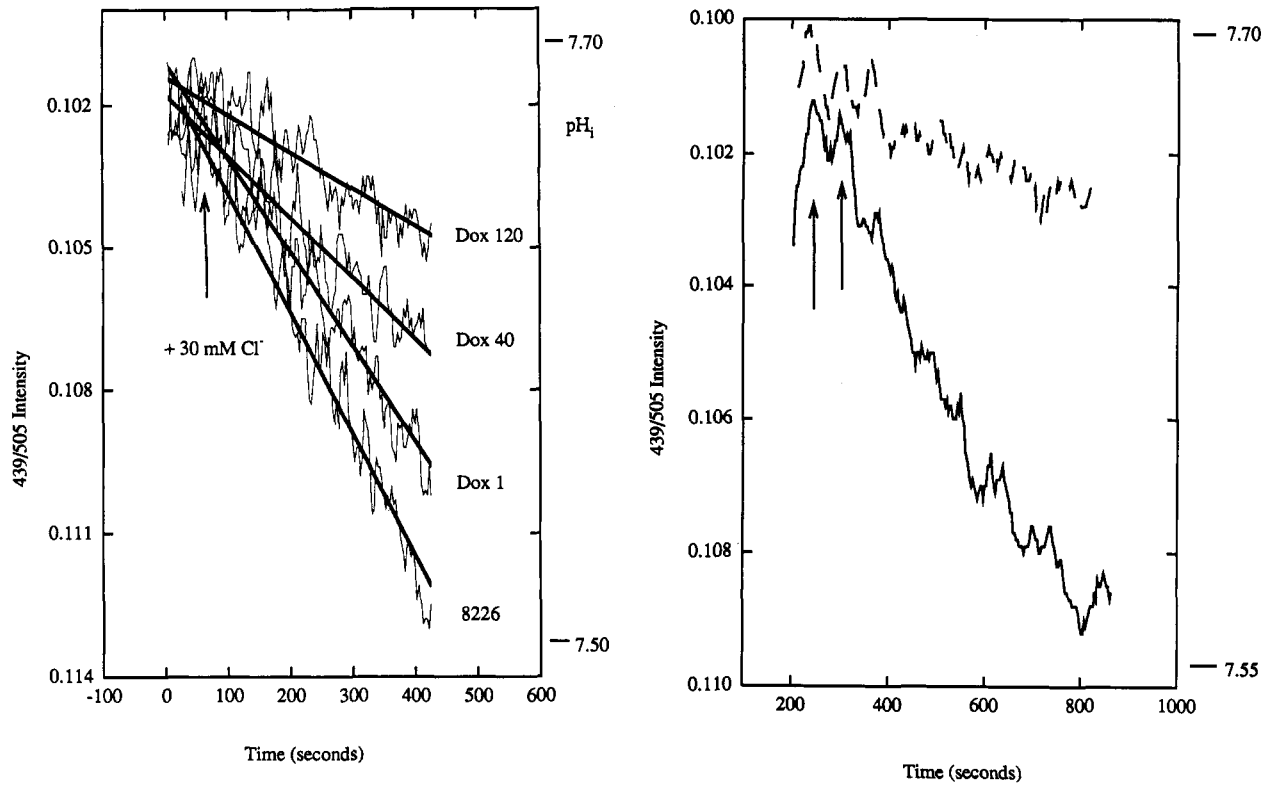

FIGURE 6: (A, left) Reacidification of (from bottom) 8226, Dox 1, Dox 40, and Dox 120 cells after alkalinization in Cl^--free media and addition of 30 mM NaCl (see Materials and Methods). The result for Dox 6 is similar to that for Dox 1 and was thus left out for ease of visual comparison. The results were essentially identical upon the addition of 30 mM choline chloride or KCl. The decrease in pH_i begins to plateau near 20 min (not shown) at pH_i higher than the normal resting pH_i, as measured in the absence of nigericin with SNARF or BCECF (see footnote 2). The arrow denotes the addition of NaCl. Raw data after 60 s are fit to a straight line; data shown are representative of at least five separate experiments. Note that although the data are noisier at pH_i 8.0–7.6 due to the poorer response of BCECF at these extrema, control pH_i *vs* 439/505-nm excitation plots are still linear (see Materials and Methods) and highly reproducible (not shown). (B, right) Reacidification for the sensitive 8226 cells before (solid line) and after (dashed line) treatment of cells with 500 μM SITS for 5 min at 37 °C. Less dramatic effects are seen with lower concentrations of SITS, supporting the participation of the AE2 isoform in this process (see also Figure 7 and Table II). The first arrow denotes the addition of BSA, the second the addition of 30 mM NaCl. Data are not smoothed.

1991), thereby exhibiting a sensitivity to stilbene inhibition that is about 2 orders of magnitude lower relative to AE1 [the erythrocyte isoform; see Kopito and Lodish (1985)]. Somewhat analogously, we observe about 70% inhibition upon the addition of 500 μM SITS (Figure 6B). Since AE2 was originally isolated from the erythroleukemic cell line K562 (Delmuth *et al.*, 1986), and subsequently from a preB lymphoblast cell line (Alper *et al.*, 1988), it is reasonable to assume that these myeloma cells (which are of B cell origin) harbor AE2.

To test this, we probed mRNA from the series of cells for expression of AE isoforms. Figure 7A,B presents the results obtained upon probing with a 2.1-kbp *Eco*RI/*Sma*I AE1 cDNA fragment (this blot was also probed for rPO) or a 2.6-kbp *Bam*HI AE2 cDNA fragment (Alper *et al.*, 1988), respectively. It is clear that the relative expression of one or more Cl^-/HCO_3^- exchangers is altered in the series of variably MDR cell lines. Thus, quantitation of the 4.3-kbp signal obtained with the AE2-specific probe (Figure 7B) shows that AE2 is overexpressed about 11-fold for the Dox 1 line relative to the 8226 line and that overexpression then *decreases* for the other members of the series, relative to Dox 1 (see Figure 7B, Table II). Somewhat analogously, probing with the AE1-specific probe reveals a unmistakable signal at 3.2 kbp for the Dox 1 line (*cf.* Figure 7A) and, amazingly, absolutely no signal for the 8226, Dox 40, or Dox 120 lines, even after continued exposure. After a 4-day exposure, trace amounts of AE1 mRNA of the same mass are seen for the Dox 6 line (not shown). Thus, although a full-length human AE2 cDNA has not yet been cloned from these cells, available data suggest that we are measuring relative levels of AE 2 activity for the 8226 line (Figure 6A) and that expression of AE2 is rather dramatically altered for one mildly resistant MDR cell line.

It is quite interesting that an mRNA of distinctly different size is revealed for Dox 1 upon probing with the AE1 fragment (Figure 7A). Since we do not see this band when we probe for AE2 (compare Figure 7A and B), it is unlikely that this band represents an alternate form of AE2 mRNA; thus, we tentatively conclude that *both* the AE2 *and* AE1 isoforms are substantially overexpressed for the Dox 1 line, whereas AE2 appears to be the only anion exchanger expressed to any appreciable level in the other lines.[5]

It is also interesting that the *increased* expression of MDR protein in the series of cells (see Table I) correlates with the *decreased* ability to recover from an alkaline shock by Cl^--dependent mechanism(s), whereas altered expression of

[5] We do not exclude the possibility that the 3.2-kbp message represents the expression of some other gene with considerable homology to AE1. The open reading frame of the 4.3-kbp mu AE1 cDNA (Kopito & Lodish, 1985) is 2.8 kbp, and that of the 4.7-kbp hu AE1 mRNA identified in fetal liver (Lux *et al.*, 1989) is about 2.9 kbp; thus, the 3.2-kbp mRNA could conceivably be encoding hu AE1. However, it is also very small relative to other isolated AE1 cDNAs from kidney, preB cells, or erythroid precursors (Alper *et al.*, 1988). Conversely, the AE2 signal we observe is about the same size as a recently identified 4.4-kbp hu "AE2" mRNA [i.e., mRNA encoding the nonerythroid and nonneuronal AE isoform (Demuth *et al.*, 1986)]. That is, to the best of our knowledge, all other AE mRNAs that have been identified are >4 kbp except for a mu AE3 from heart [3.4 kbp; see Kopito *et al.* (1989)] and an unidentified AE from rat stomach [3.6 kbp; see Kudrycki *et al.* (1990)]. Thus, the 3.2-kbp AE1 signal represents a novel transcript in these human MDR cells.

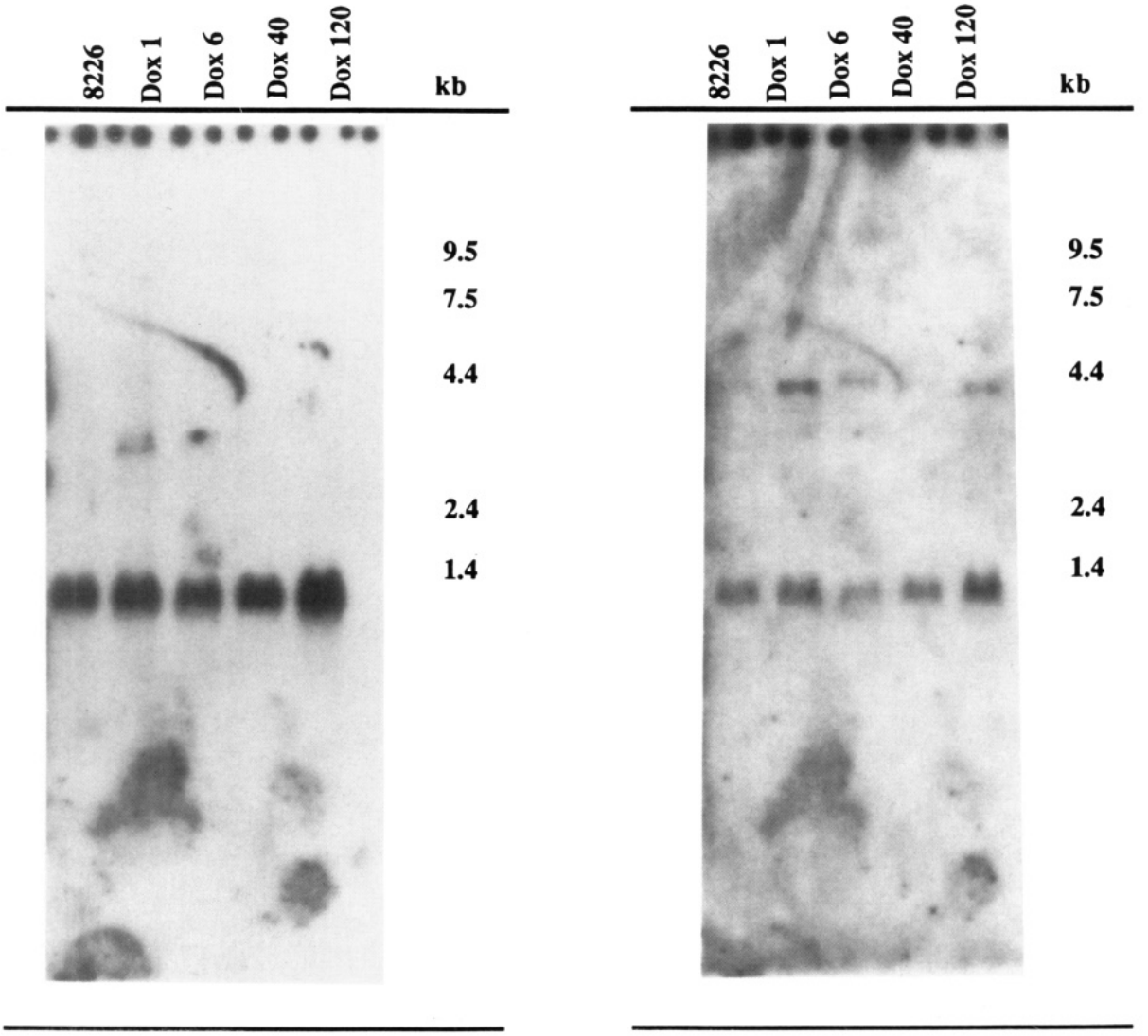

FIGURE 7: (A, left) Northern blot analysis of relative AE1 expression. Note the prominent band at 3.2 kbp for the Dox 1 mRNA, but its conspicuous absence in the other lanes. The blot was previously probed for rPO to verify the integrity of the mRNA (note the clear band at 1.4 kbp with no smearing). Exposure time was 48 h. Additional blots (not shown) using different mRNA preparations that also exhibited no evidence of degradation failed to identify AE1 mRNA in the 8226, Dox 40, or Dox 120 lanes as well, even after drastic overexposure; however, trace AE1 could be seen for Dox 6 after prolonged exposure. (B, right) Northern blot analysis of relative AE2 expression. Note the prominent band at 4.3 kbp, which is most intense for the Dox 1 line. The blot probed in A was stripped (see Materials and Methods) and reprobed with the AE2 cDNA. Note the absence of the 3.2-kbp AE1 band. Relative AE2 intensities were quantitated as described in Materials and Methods and are summarized in Table II. Exposure time was 48 h.

AE2 does not (compare Figure 7A,B and Tables I and II). This is in contrast to the strong positive correlation between the rate of Na^+-dependent realkalinization and the relative expression of NHE for the series (compare Table II and Figure 4).

Effects of Medium HCO_3^- on pH_i. As a further qualitative examination of pH_i homeostasis, changes in pH_i were assessed for cells in media of similar pH that did or did not contain HCO_3^-. Figure 8 shows that, after 27 mM HCO_3^- is replaced in the incubating medium with 20 mM HEPES and equilibrated for 10–15 min, pH_i increases for the sensitive cells by nearly 0.4 unit, as might be expected upon the loss of Cl^-/HCO_3^- exchange-mediated intracellular acidification ability (compare pH_i at time zero for the solid and dashed thin lines).

In contrast, similar experiments with resistant Dox 120 cells reveal that the removal of HCO_3^- has little effect on pH_i (compare pH_i at time zero for the solid bold lines) and may even lead to mild intracellular acidification. Relative changes in pH_i upon the removal of HCO_3^- appear to correlate to some extent with the relative expression of MDR protein in the series of MDR cells (not shown) and will be examined in more detail in a future report.

Titrating pH_o leads to smaller compensatory changes in pH_i for both cell types (Figure 8); however, pH_i of the resistant cells in the absence of HCO_3^- (bold dashed line) appears to be slightly less perturbed upon alteration of pH_o (compare to bold solid), whereas the converse is true for sensitive cells (compare dashed thin to solid thin lines). Thus, when pH_o is titrated to 6.90 by the addition of HCl (first arrow), resistant cells in the presence of HCO_3^- (solid bold line) exhibit a pH_i about 0.25 unit lower than that at pH_o 7.33 (*cf.* Figure 8). Sensitive cells, on the other hand, exhibit a pH_i only 0.09 unit lower (solid thin line) in the presence of HCO_3^- upon titration to 6.90, whereas in the absence of HCO_3^- a much larger change is seen. This pattern is repeated upon the titration of pH_o to 6.60 (second arrow). Qualitatively, it is as if the resistant cells in the presence of HCO_3^- behave like sensitive cells in the absence of HCO_3^- (compare solid bold and dashed thin lines).

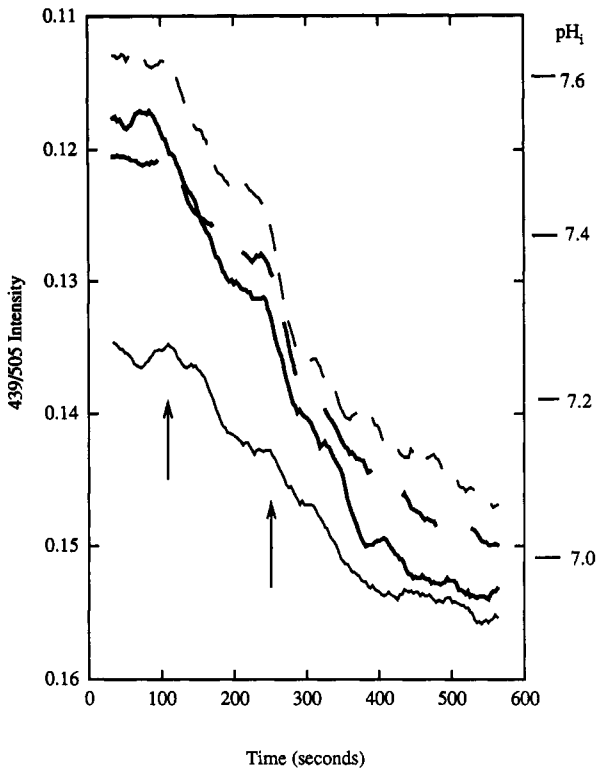

FIGURE 8: Effect of the removal of HCO_3^- on steady-state pH_i and response to pH_o alterations for the resistant Dox 120 cells (bold lines) and the sensitive 8226 cells (thinner lines). Replacement of RPMI media with HBSS containing 20 mM HEPES and no HCO_3^- (pH 7.33) (thin dashed line) results, after 10 min (zero time in this Figure), in substantial alkalinization of sensitive 8226 cells, whereas replacement with balanced salts containing 27 mM HCO_3^- and no HEPES (pH 7.33) resulted in only slight alkalinization (thin solid line). Conversely, resistant Dox 120 cells became slightly more acidic (bold dashed line) when HCO_3^- was removed. The HCO_3^--containing buffer was equilibrated with 5% CO_2, and the cuvette was continuously purged when pH_o 7.33 was desired. The arrows designate the titration of pH_o to 6.90 and 6.60, respectively. The plateaus reached immediately before the arrows are reasonably flat for 10–15 min if further titration is not attempted (not shown). Note that, upon titration of pH_o, 8226 cells better maintain pH_i in the presence of HCO_3^-, whereas the opposite is true for Dox 120 cells. Data shown are representative of three separate experiments. Data are smoothed as for Figure 1.

Altered Electrical Membrane Potential. Since an elevated steady-state pH_i would perturb the electrochemical membrane potential ($\Delta\mu_{H^+} = \Delta\Psi + \Delta pH$), we examined the relative magnitude of $\Delta\Psi$ for the series of 8226-derived cells. Additional impetus for these experiments comes from the observation that many drugs in the "MDR spectrum" are lipophilic cations and the fact that the intracellular/extracellular distribution of lipophilic cations is highly dependent on $\Delta\Psi$.

We first tested whether the K^+ permeability of these cell membranes was dominant with respect to determining $\Delta\Psi$, since analysis of the relative signal from $\Delta\Psi$-sensitive fluorometric dyes upon the addition of valinomycin in media of various $[K^+]$ [*i.e.*, the K^+/valinomycin null point method; see Laris and Hoffman (1986)] is a convenient approach for estimating $\Delta\Psi$. Figure 9 shows that the relative change in 100 nM bis-oxonol fluorescence is greater when resistant Dox 40 cells are diluted into medium containing either 145 mM Na^+ and 0 mM K^+ or 145 mM K^+ and 0 mM Na^+, relative to an identical number of 8226 cells. Although only qualitative, this indicates that less anionic dye is excluded from the resistant cells, perhaps because they maintain a lower $\Delta\Psi$. In any case, upon addition of the K^+ ionophore valinomycin (10 μM, downward arrows) or the Na^+/K^+ ionophore gramicidin (1.5 μM, upward arrows), the relative changes in oxonol fluorescence are very similar for the different cells. In low $[K^+]$/high $[Na^+]$ solution, the addition of valinomycin leads to a positive change in oxonol fluorescence as the cell is hyperpolarized, whereas a negative change (depolarizing) is seen when the cells are in high K^+ buffer. When gramicidin is added 100 s after the addition of valinomycin, a depolarizing signal of very similar relative magnitude is seen for both cell types in high $[Na^+]$, but virtually no change is seen for the cells in high $[K^+]$, illustrating that P^K is dominant with respect to $\Delta\Psi$ (there is in fact a very slight positive signal for the resistant cells in high $[K^+]$ upon the addition of gramicidin, perhaps indicating a slightly different contribution of P^{Na} to $\Delta\Psi$). When gramicidin is added before valinomycin for cells at high $[K^+]$ (not shown), very similar data are obtained. Similar data in all experiments are obtained with the cationic dye $diSC_3(5)$ (not shown), although the direction of the intensity changes upon addition of the ionophores is of course opposite.

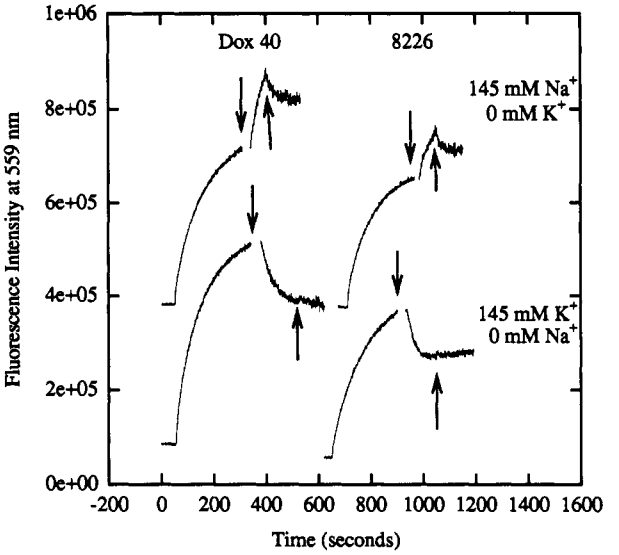

FIGURE 9: Fluorescence of 100 nM bis-oxonol upon the addition of exactly 1.0×10^6 Dox 40 (left side) or 8226 (right side) cells to oxonol/HBSS harboring high $[Na^+]$ (top) or high $[K^+]$ (bottom). Departure from the flat base line indicates the addition of cells, and downward- and upward-directed arrows denote the addition of 10 μM valinomycin and 1.5 μM gramicidin, respectively. Note that the base-line change induced by the interaction of oxonol in solution with added valinomycin was subtracted out for ease of visual comparison (the base-line change is instantaneous and easily identifiable). Note that both cell types in high $[K^+]$ exhibit substantial depolarization upon the addition of valinomycin and virtually no change upon subsequent addition of gramicidin, whereas the converse is true for both cell types in high $[Na^+]$ HBSS. Although not shown, the positive (hyperpolarizing) signal in the top two traces plateaus slowly (300–500 s after addition of valinomycin); gramicidin was added 100 s after the addition of valinomycin in order to be consistent with the bottom two traces. The addition of gramicidin *before* the addition of valinomycin in high $[Na^+]$ gives a depolarizing signal of very similar relative magnitude for both cell types (not shown). Note that similar data are also obtained for the other cell lines using either oxonol or $diSC_3(5)$ (not shown); the presented data are representative of three separate experiments.

A qualitative appreciation of rather dramatic changes in $\Delta\Psi$ for the different cells can be obtained by examination of the $diSC_3(5)$ fluorescence traces presented in Figure 10. In these experiments, it is conspicuous that the overall change in $diSC_3(5)$ fluorescence for the different cell types decreases steadily for cells of increasing resistance, suggesting that electrical potential is reduced as resistance increases. This is because $diSC_3(5)$ fluorescence changes are proportional to

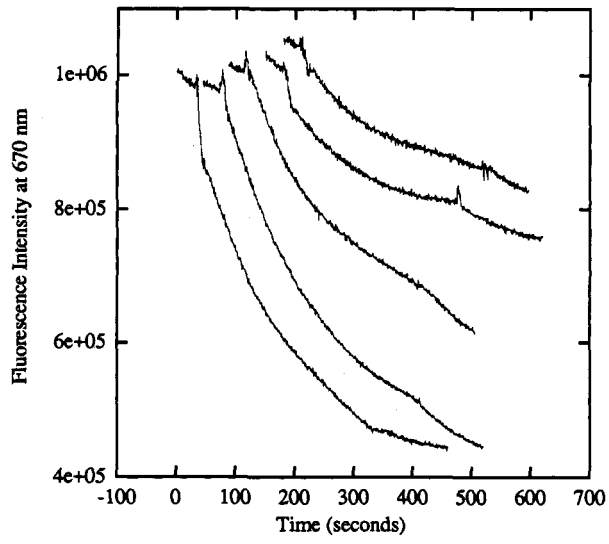

FIGURE 10: Relative fluorescence of 50 nM $diSC_3(5)$/HBSS (pH 7.33) upon the addition of exactly (from left) 5.0×10^5 8226, Dox 1, Dox 6, Dox 40, or Dox 120 cells. $[K^+]_o$ was 10 mM, and 10 μM valinomycin was added 300 s after the addition of cells. Note the dramatically lower efficiency of internalization of the $\Delta\Psi$ probe for the MDR cells and the steady trend correlating with resistance. Data shown are representative of many separate experiments. Solutions of exactly the same volume and dye concentration were equilibrated to exactly the same temperature, exactly the same number of cells (5.0×10^5) was added, and the suspension was mixed for exactly the same amount of time. Note that these cell lines are all derived from one another and are of approximately the same size (Table I).

intracellular partitioning of the cationic dye, which is in turn directly proportional to the magnitude of $\Delta\Psi$ (negative inside). The pH_i differences between these cells (Table I) are unlikely to lead to differences of the magnitudes observed. Although it could also be proposed that dye association is lower for the resistant cells because MDR protein expressed in these cells is actively extruding the dye, we have determined that this hypothesis is unlikely (see below and the Discussion).

To quantitatively estimate $\Delta\Psi$, two approaches were followed using two different dyes, $diSC_3(5)$ and di-4-ANEPPS. First, the size of the $diSC_3(5)$ fluorescence intensity change upon the addition of valinomycin to cells in media of different $[K^+]$ was measured and plotted *vs* $[K^+]_o$ to determine graphically the null point (see Figure 11A) for the different cells (see Table III). By inserting the null point concentration of $[K^+]_o$ into the Nernst relation $[E = -nRT\ln([K^+]_i/[K^+]_o)]$, one can calculate $\Delta\Psi$ if $[K^+]_i$ is known. Toward this end, we first verified that the relative volume of cells in the series was similar (Table I) by determination of the mean particle size of cell suspensions *via* Coulter sizing (see Materials and Methods). We also verified that members of the series had similar internal water volume (Table I) by measuring [^{14}C]-inulin/^3H_2O ratios in the pellet and supernatant of cell suspensions that were incubated with the compounds and then centrifuged (see Materials and Methods). Thus, although both methods merely yield estimates of cell volume, comparison between determinations allow us to conclude that V_i is similar for most of the different cells; however, note that V_i for the Dox 6 line is somewhat smaller.

Flame photometry of HNO_3 extracts from dried cell pellets (2.0×10^7 cells) reveals that the total cell-associated K^+ is 0.1067, 0.1101, 0.0960, 0.1080, and 0.1096 mmol/l $\times 10^6$ cells for the 8226, Dox 1, Dox 6, Dox 40, and Dox 120 cell lines, respectively. Thus, although an exact determination of osmotically sensitive $[K^+]_i$ is of course difficult, it is reasonable to assume that $[K^+]_i$ is similar for the different cell lines. $[K^+]_i$ values based on estimated water V_i and these K^+ determinations are listed in Table I.[6]

We observe that differences between the $diSC_3(5)$ null points for the different cells are large (Table III); thus, differences in calculated $\Delta\Psi$ are significant (*cf.* Table III). $[K^+]_i$ would have to increase, for example, from about 160 mM (the estimated value for 8226 cells) to greater than 900 mM for the Dox 6 cells for there to be no appreciable difference in calculated $\Delta\Psi$ for the two cell lines (see also the Discussion).

To test the measured trend in $\Delta\Psi$ alterations, we also plotted the relative change in the ratio of 440/505-nm excitation for cells incubated with di-4-ANEPPS for 60 s in media of various $[K^+]_o$ upon the addition of 10 μM valinomycin (see Figure 11B), and these results are also tabulated in Table III. The magnitude of the change is small upon the addition of valinomycin, and we thus found this method to be less quantitative; however, a similar trend in terms of decreased $\Delta\Psi$ for the increasingly resistant cells is also seen (*cf.* Table III), further supporting the data obtained with $diSC_3(5)$. Furthermore, since di-4-ANEPPS is a very fast response "ratiometric" dye [*i.e.*, the *ratio* of two excitation wavelengths is plotted *vs* $[K^+]_o$ instead of the change at one wavelength, as is the case for $diSC_3(5)$], differences in dye concentration for various cells are much less of a concern, and the measured differences between the different cell lines cannot be due to any postulated altered transport of the dye.

Interestingly, when we plot $\Delta\Psi$ (average of the two estimates in Table III) and ΔpH for the cells *vs.* log doxorubicin resistance, we find that the decrease in $\Delta\Psi$ parallels the increase in chemical energy associated with increased ΔpH (Figure 12). The "exchange" of $\Delta\Psi$ for ΔpH is nearly stoichiometric, such that the overall electrochemical membrane potential ($\Delta\mu_{H^+}$) is reasonably constant (see Table III and Figure 12). Note also the strong inverse correlation between MDR protein expression (*cf.* Table I) and $\Delta\Psi$ in the series of MDR cells.

DISCUSSION

These data can be summarized as follows: (1) NHE activity as measured in transient assays is increased for MDR cells relative to the sensitive parent. The rate of Na^+-induced recovery from an acid shock qualitatively correlates with the relative level of Na^+/H^+ exchanger mRNA in the series of increasingly MDR cells, but steady-state pH_i does not. Increased NHE activity for the resistant cells is affected by preincubation with 10–25 μM verapamil for 10–30 min, but not by the addition of verapamil with Na^+. We find only small differences in NHE activity under steady-state conditions for the different cell lines (not shown); a more detailed discussion of this as well as steady-state AE2 activity (see below) will be published elsewhere.

(2) Cl^--dependent reacidification after transient intracellular alkalinization is impaired in these MDR cells. The concentration of SITS required to completely inhibit reacidification for the sensitive cells is consistent with the presence of the AE2 isoform, as is Northern blot analysis with AE1- and AE2-specific probes. Relative expression of AE does not correlate with the ability to reacidify; however, relative expression of MDR is inversely correlated. The behavior of MDR *vs* sensitive cells in media ± HCO_3^- further suggests

[6] In general agreement with these data, all other previously published values of $[K^+]_i$ for lymphocytes have varied between 120 and 170 mM (Iverson, 1976; Rink *et al.*, 1980; Grinstein & Dixon, 1989).

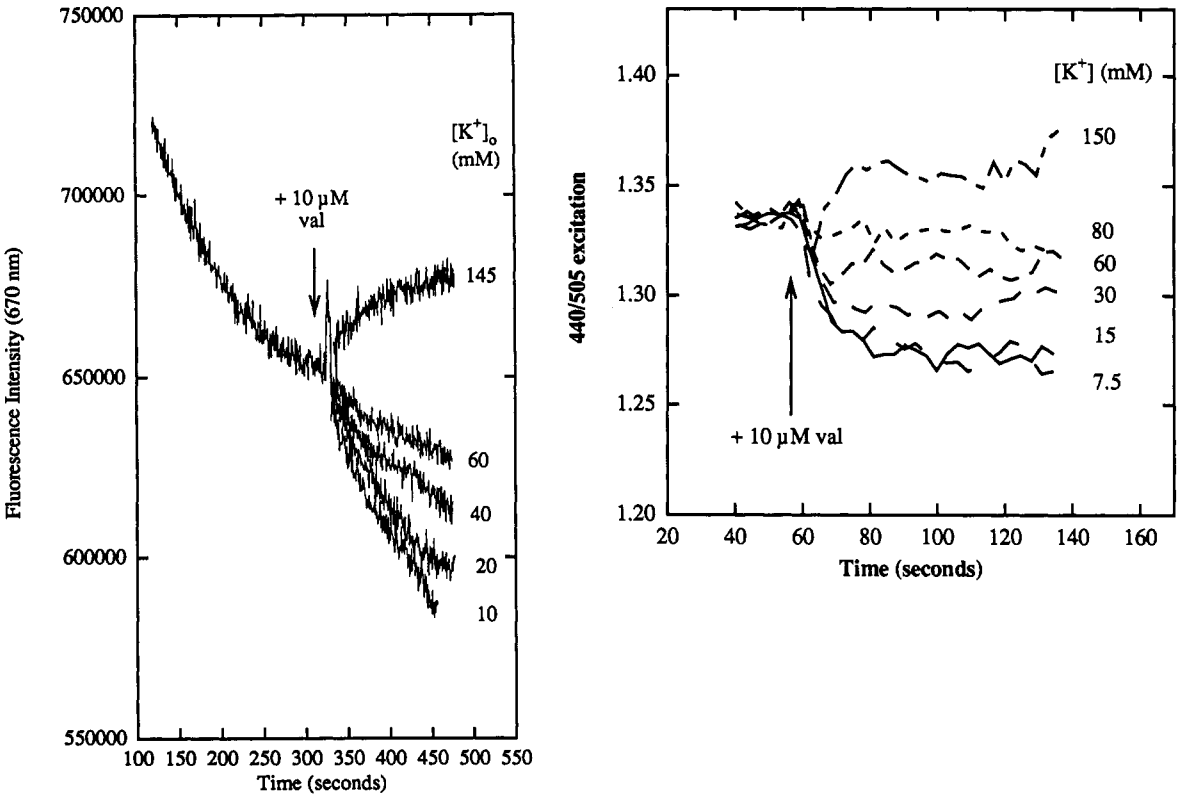

FIGURE 11: (A, left) K^+/valinomycin determination of the null point for Dox 120 cells equilibrated with 50 nM $diSC_3(5)$ as described. Samples of 5×10^5 cells were diluted into $diSC_3(5)$/HBSS harboring (from bottom) 10, 20, 40, 60, or 145 mM K^+, and equilibration was achieved in about 5 min. Then 10 μM valinomycin was added, and the resultant jump in fluorescence was noted. Base lines before the addition of valinomycin for the different curves were superimposed before comparing the curves after the addition of valinomycin. The base line before the addition of valinomycin was extrapolated out by curve fitting, so that this "base-line" slope could be accounted for when calculating the change in fluorescence. The average of several plots of $[K^+]_o$ *vs* fluorescence intensity change were used to determine the null point and thus quantitatively estimate $\Delta\Psi$ (see Table III). (B, right) K^+/valinomycin determination of the null point for Dox 120 cells using the ratiometric styryl dye di-4-ANEPPS (see Materials and Methods). Experiments were performed essentially as described for $diSC_3(5)$, (see part A) except that only 60 s was required for equilibration before the addition of valinomycin. Localization of di-4-ANEPPS during the time course of the measurements was predominantly to the plasma membrane as witnessed by fluorescence microscopy (not shown). The reasonably flat region between 90 and 140 s for each curve was fit by a straight line in order to compute the difference in excitation ratios for the curves before and after the addition of ionophore; these were then plotted *vs* $[K^+]_o$ to determine the null point. As also determined recently by Loew and colleagues (Montana *et al.*, 1989; Loew *et al.*, 1993), plots of ANEPPS excitation ratios *vs* potential are well behaved between +10 and −100 mV. Note the reasonably good agreement between the determination of the null point by this method *vs* the $diSC_3(5)$ method (see Figure 11A and Table III).

Table III [a]

	null point (mM K^+)		estimated $\Delta\Psi$ (mV)			
cell line	$diSC_3(5)$	di-4-ANEPPS	$diSC_3(5)$	di-4-ANEPPS	ΔpH (mV) (pH 7.30)	$\Delta\mu_{H^+}$ (mV) (= $\Delta\Psi$ + ΔpH)
8226	7.2	22	−81[b]	−52	+11	−56
Dox 1	12	35	−67[b]	−39	+0.5	−53
Dox 6	59	50	−29	−30	−6.5	−38
Dox 40	74	80	−19	−21	−14.8	−33
Dox 120	72	85	−19	−20	−19.5	−37

[a] K^+/valinomycin null point was determined graphically by plotting the relative change in the 610-nm fluorescence intensity (for $diSC_3(5)$) or the ratio of 440/505-nm excitation (di-4-ANEPPS) *vs* $[K^+]_i$ listed in Table I. Note that $\Delta\Psi$ calculated for the 8226 cells agrees reasonbly well with the $\Delta\Psi$ previously measured for lymphocytes by similar methods (Grinstein & Dixon, 1989). $\Delta\mu_{H^+}$ was calculated using the average of the $\Delta\Psi$ values obtained by the $diSC_3(5)$ and di-4-ANEPPS experiments; recall (Rottenberg, 1976) $\Delta\mu_{H^+}/F = \Delta p = \Delta\Psi - Z\Delta pH$, where F is the Faraday constant, $Z = 2.3RT/F = 59$ mV, and ΔpH is $pH_i - pH_0$. [b] Since the $diSC_3(5)$ measurement is made in minutes, these estimates may be slightly high due to a contribution from mitochondria, and this increase would be larger for cells with larger plasma membrane $\Delta\Psi$ due to higher cytoplasmic $[diSC_3(5)]$. Note that the ANEPPS values cannot be affected in this way because the dye is extremely well localized to the plasma membrane in the 60–90 s required for the measurement (see Materials and Methods).

that HCO_3^--dependent pH_i homeostasis is altered in these MDR cells. We are unable at this time to determine unequivocally whether AE2 activity under steady-state conditions is altered in these cells, presumably because of the low sensitivity to various stilbene inhibitors. In any case, we feel it is provocative that *increased* AE expression is seen for cells that exhibit a *decreased* ability to *reacidify* in a Cl^--dependent manner, since AE activity is often found to *lower* pH_i.

(3) Electrical membrane potential ($\Delta\Psi$) is dramatically altered in these MDR cells, as evidenced by measurements with cationic ($diSC_3(5)$), anionic (bis-oxonol), and ratiometric (di-4-ANEPPS) probes. Quantitative estimates of the magnitude of $\Delta\Psi$ by the null point method reveal that $\Delta\Psi$ decreases as resistance and MDR protein expression increase. However, notably, the chemical energy associated with increased ΔpH (due to elevated pH_i in these cells) apparently compensates

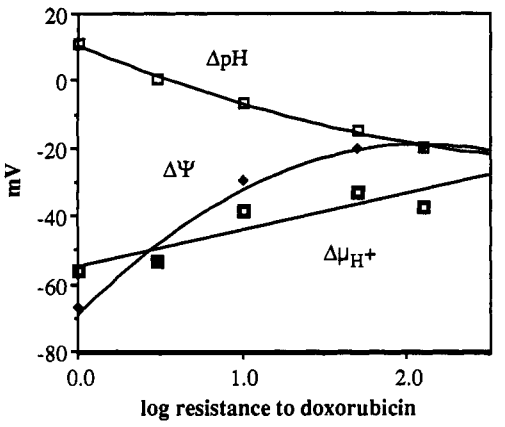

FIGURE 12: Plot of ΔpH, ΔΨ, and $\Delta\mu_{H^+}$ *vs* log resistance of the cells in the series. Note the reciprocal relationship between the trends for ΔΨ and ΔpH and the much less dramatic change in $\Delta\mu_{H^+}$. The ΔΨ and ΔpH data were fit by a quadratic, and the $\Delta\mu_{H^+}$ data were fit by a straight line. Note that, if only the di-4-ANEPPS values for ΔΨ are used to compute $\Delta\mu_{H^+}$, the $\Delta\mu_{H^+}$ curve is essentially flat.

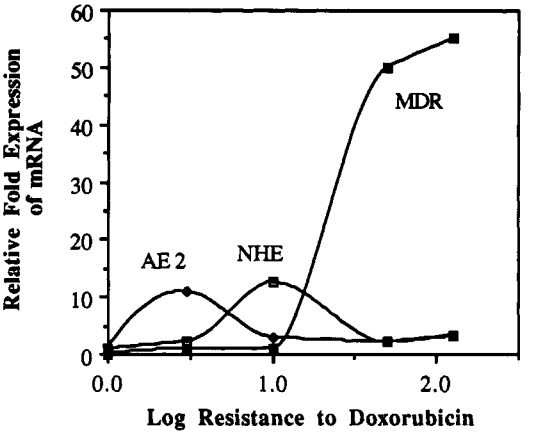

FIGURE 13: Plot of the relative expression of AE2, NHE, and MDR mRNA *vs* log resistance for the different cells. Note the sequence of overexpression and the apparent mutual exclusion of the different mRNAs. Although very low levels of MDR mRNA are found for the Dox 6 line, measurable protein is seen by Western blot [see Table I and Dalton *et al.* (1989)].

for the loss of electrical potential, such that the overall electrochemical membrane potential remains similar.

In terms of the validity of our ΔΨ measurements, several points deserve mention: (1) Agreement in the *trends* observed with the carbocyanine $diSC_3(5)$ and styryl di-4-ANEPPS methods suggests that altered signals for the carbocyanine are *not* due to any active transport of the dye; recall that di-4-ANEPPS is a ratiometric probe of potential. Furthermore, we do not find any difference in the *rate* of efflux of $diSC_3(5)$ from these different cells (not shown). Thus, no evidence for active transport of $diSC_3(5)$ exists, at least for this series of cell lines, since increased expression of a putative active transporter should lead to rate enhancement in active transport of the putative substrate [see Roepe (1992) for a discussion of rate *vs* steady-state effects]. Recall also that these probes absorb and fluoresce at very different wavelengths, severely limiting the spectrum of possible optical artifacts that could in anyway conceivably mimic the observed behavior of *both* dyes in the *same* way. (2) Our quantitation of ΔΨ is dependent on $[K^+]_i$, which is only estimated in this work. However, we are fairly confident that $[K^+]_i$ does not *change* dramatically between different cell types; thus, in terms of the *trend* in ΔΨ values calculated from the Nernst relation, the point is moot. (3) K^+/valinomycin titration also assumes that the K^+ *current* is dominant with respect to determining ΔΨ; we have made empirical measurements for the different cells that support this (*cf.* Figure 9) using both anionic and cationic dyes, but more work is needed to quantitate precisely any altered Cl^- or Na^+ (or K^+ for that matter) currents in these cells under physiological conditions before the estimated differences in ΔΨ are completely reliable. Thus, although it is entirely appropriate to conclude that ΔΨ is decreased in MDR cells and that it decreases concomitant with increased MDR and increased MDR protein expression, determination of the exact magnitude of the differences between different cells awaits further study.

Notably, however, our data are in substantial agreement with recent work of Gupta and colleagues (Vayuvegula *et al.*, 1988) as well as that of Lampidis and co-workers (Hasmann *et al.*, 1989). Both groups concluded that ΔΨ is decreased in MDR cells by virtue of dye exclusion in fluorescence-activated cell sorting (FACS) experiments. Although trends in series of MDR cells expressing variable MDR protein were not examined in either study, nor was any attempt made to quantitatively estimate ΔΨ, their observation of lower dye retention is consistent with our estimates of reduced ΔΨ in MDR cells.

Figure 13 plots the relative expression of hu MDR 1, AE2, and NHE mRNA for the series of cells *vs* log relative resistance (relative AE1 is not plotted since we have no signal for 8226; thus overexpression is essentially infinite). There are several important points: (i) increased pH_i does not correlate with increased expression of AE or NHE (or their ratio), but does appear to correlate with MDR protein expression, as does decreased ΔΨ (compare to Figure 12 and Table I); (ii) at clinically relevant levels of MDR (3–10 fold), the overexpression of AE and NHE is more dramatic than the overexpression of MDR in these cells; (iii) a pattern of transporter gene overexpression appears wherein AE appears to be dramatically overexpressed first, followed by NHE and then MDR. It is as if the significant overexpression of one gene excludes the overexpression of the other two, *i.e.*, as they develop increased drug resistance, overexpression of AE, NHE, and MDR genes in this series of MDR cells is mutually exclusive.

Thus, although we have not ruled out all other possible mechanisms of altered pH_i homeostasis, we propose that intracellular alkalinization of MDR cells is at least partly due to the expression of MDR protein, since neither the trend in altered AE nor NHE expression (or, importantly, the *ratio* of these trends) correlates with elevated pH_i, but increased MDR protein expression apparently does (compare Tables I and II). That is, the altered expression of other transporters critically involved in pH_i regulation (NHE and AE) in and of themselves does not easily explain the observed elevation of steady-state pH_i for MDR cells although they may play a role, particularly early on in the development of resistance. In support of this idea, our laboratory (P. D. Roepe and D. Carlson, unpublished results) and one other (Thiebaut *et al.*, 1989) have noted that, upon transfection of NIH 3T3 cells with hu MDR 1 cDNA, the cells exhibit a pH_i 0.10–0.20 unit more alkaline relative to control transfectants, even though the cells were never exposed to chemotherapeutics. Although more detailed work remains to be done, it is unlikely that this is due to the altered expression of NHE and/or AE (L.-Y. Wei and P. D. Roepe, unpublished results).

Since increased expression of the MDR protein apparently leads to decreased ΔΨ as well as increased pH_i, these MDR cells harbor a powerful "one–two punch" against a wide variety of toxic hydrophobic cations and weak bases and/or drugs

that bind to intracellular targets in a highly pH_i-dependent manner. Thus, elevated pH_i will lead to decreased ionic sequestration of hydrophobic weak bases and lower the efficiency of binding for drugs that react with targets in a highly pH-dependent fashion. It may also lower the availability of drug target in some cases, as discussed previously (Roepe, 1992), further lowering the statistical likelihood of sequestration. Lower electrical potential will lead to lower intracellular levels of hydrophobic cations [see also Gros *et al.* (1992)] as is well appreciated. In fact, distribution of lipophilic cations is a well-known method for *quantitating* $\Delta\Psi$, assuming it does not change during the time necessary for cation equilibration [see Rottenberg (1979)]. We also speculate that significant perturbations in $\Delta\Psi$ might alter the rate of passive membrane translocation of some large, uncharged, hydrophobic molecules such as colchicine, although direct physical measurements are required to test this [see El-Mashak & Tsong (1985)]. Finally, a different ΔpH can alter leaflet distribution of phospholipids in bilayers (Hope *et al.*, 1989), and this might lead to subtle changes in the affinity of compounds such as colchicine for a particular side of the membrane.

We propose that, within the plasma membrane environment of these cells, the molecular-level function of MDR protein is essentially to "exchange" the energy stored as $\Delta\Psi$ for an induced ΔpH, thus conferring broad resistance to a variety of hydrophobic weakly basic compounds and lipophilic cations, as well as compounds that bind to intracellular targets in a highly pH-dependent manner. This model is intuitively more satisfying to us than the active drug–transporter hypothesis because it obviates the need for a transporter specifically binding and transporting many structurally diverse chemotherapeutics and thus adheres to Mitchellian chemiosmotic theory, a touchstone of molecular membrane transport. The model is also in some agreement with other recent, independently obtained data [see Valverde *et al.* (1992) and Gill *et al.* (1992)], which show that MDR protein expression leads to the introduction of novel Cl^- permeabilities across the plasma membrane. Cl^- translocation by the MDR protein could indirectly raise pH_i by influencing the distribution of Cl^- and/or HCO_3^- in some cells, although more information pertaining to the function of AE isoforms (*i.e.*, K_m for Cl^- and the effects of $\Delta\Psi$, etc.) as well as their expression in MDR cells is required to explain why Cl^- translocation by MDR protein does not lead to *acidification* of pH_i in some cases, as might also be predicted.

In any case, since eukaryotic plasma membranes normally exhibit low permeability to anions, novel Cl^- permeabilities introduced by MDR protein might also have significant effects on $\Delta\Psi$, although it is difficult to predict the magnitude of the effect for a particular cell type without more data. That is, since $\Delta\Psi$ is the sum of a series of terms, each being the concentration gradient multiplied by the membrane permeability of a charged species, alterations in the *permeability* for ions exhibiting large concentration gradients across the plasma membrane (*i.e.*, Na^+, K^+, and Cl^-) have nonnegligible effects. In particular, decreased $\Delta\Psi$ could be associated with decreased K^+ current or increased Cl^- current for many eukaryotic cell types.

Although one interpretation of other recent data (Gill *et al.*, 1992) is that the MDR protein must be *both* an active drug transporter *and* a Cl^- channel, in the absence of direct active drug transport data in the form of unequivocal evidence for drug transport against a significant concentration gradient (where volume, pH_i, and/or $\Delta\Psi$ alterations have also been eliminated as explanations for altered accumulation or efflux) and/or significant rate enhancement in the drug efflux process [where rate is measured under conditions where *exchangeable* drug is the same; see Roepe (1992)], we feel the altered pH_i/$\Delta\Psi$ "one–two punch" model for MDR protein is the more attractive.

All mechanisms that lower the efficiency of intracellular partitioning will lower the statistical likelihood that drug will react with target. However, different mechanisms have different efficiencies for different drugs. Implicit in the one–two punch model is the great degree of "resistance heterogeneity" exhibited by different cells expressing similar levels of MDR protein, as well as their different "resistance profiles" (*i.e.*, ranked preferential resistance to various drugs). The retention of different drugs with different pK_b's and targets will be affected differently by similar pH_i and $\Delta\Psi$ perturbations (*i.e.*, retention of doxorubicin is affected by both $\Delta\Psi$ and pH_i, whereas retention of colchicine is probably affected more by pH_i). Since different cells have different NHE and AE isoforms, different resting $\Delta\Psi$ and pH_i, and different priorities in terms of maintaining these values, it is not trivial to predict the magnitude of pH_i or $\Delta\Psi$ alterations produced by a given amount of MDR protein translocating a given amount of Cl^-.

Finally, mutant MDR proteins having decreased Cl^- translocation efficiency may lower $\Delta\Psi$ and raise pH_i by different degrees (P. Gros and P. D. Roepe, unpublished data). Since relative resistance to a given drug *vs* $\Delta\Psi$ or *vs* pH_i plots are not linear (P. D. Roepe and S. Basu, unpublished data), mutants with partial ion translocating ability will likely alter the resistance profile of a transfected cell, relative to a cell transfected with the wild type. Thus, the model predicts that the cellular context of MDR overexpression is critical. Different cells have different resting $\Delta\Psi$ and pH_i and different isoforms of NHE and AE, and these will likely impact on ion translocation by MDR protein. We argue, basically, that they are potentially as important for determining the MDR phenotype in some cells as MDR protein expression.

ADDED IN PROOF

Recently (J. Luz, P. Gros, and P. D. Roepe, unpublished results), we have verified by single cell photometry methods that Cl^-/HCO_3^- exchange is perturbed upon transfecting LR73 fibroblasts with either wild-type murine MDR 1 or MDR 3, but not upon transfecting with MDR mutants unable to confer MDR (manuscript in preparation).

ACKNOWLEDGMENT

The authors thank Subham Basu, Dr. Gustavo Frindt, Kirk Pabon, and Tom Delohery for help with tissue culture, flame photometry, β quantitation, and Coulter sizing, respectively; Drs. Olaf Andersen, Larry Palmer, and Randi Silver (Cornell University Medical College), Dr. Kathy Scotto (Sloan-Kettering Institute), and Dr. Leslie Loew (University of Connecticut Health Center) for helpful discussion; Dr. William S. Dalton (University of Arizona Cancer Center) for the cell lines used in this work; Dr. Sergio Grinstein (Hospital for Sick Children, Toronto, Ontario, Canada) for investigating the immunoreactivity of NHE in our plasma membrane preparations and for helpful discussion; and Drs. Ron Kopito (Stanford University) and Jacques Pouysségur (Université de Nice) for providing us with cDNA probes for anion exchangers and Na^+/H^+ antiporter, respectively. P.D.R. also thanks Dr. Kopito for educating him with respect to the different behavior of AE isoforms.

REFERENCES

Alper, S., Kopito, R. R., Libresco, S. M., & Lodish, H. F. (1988) *J. Biol. Chem. 263*, 17092–17099.

Beck, W. T., Cirtain, M. C., & Lefko, J. L. (1983) *Mol. Pharmacol. 24*, 485–492.

Biedler, J. L., & Rheim, H. (1970) *Cancer Res. 30*, 1174–1184.

Boscoboinik, D., Gupta, R. S., & Epand, R. M. (1990) *Br. J. Cancer 61*, 568–572.

Chomczynski, P., & Sacchi, N. (1987) *Anal. Biochem. 162*, 156–159.

Cole, S. P. C., Bhardwaj, G., Gerlach, J. H., Mackie, J. E., Grant, C. E., Almquist, K. C., Stewart, A. J., Kurz, E. U., Duncan, A. M. V., & Deeley, R. G. (1992) *Science 258*, 1650–1654.

Cornwell, M. M., Safa, A. R., Felsted, R. L., Gottesman, M. M., & Pastan, I. (1986) *Proc. Natl. Acad. Sci. U.S.A. 83*, 3847–3850.

Dalton, W. S., Durie, B. G. M., Alberts, D. S., Gerlach, J. H., & Cress, A. E. (1986) *Cancer Res. 46*, 5125–5130.

Dalton, W. S., Grogan, T. M., Rybski, J. A., Scheper, R. J., Richter, L., Kailey, J., Broxterman, H. J., Pinedo, H. M., & Salmon, S. E. (1989) *Blood 73*, 747–752.

Demuth, D. R., Showe, L. C., Ballantine, M., Palumbo, A., Fraser, P. J., Cioe, L., Rovera, G., & Curtis, P. J. (1986) *EMBO J. 5*, 1205–1214.

El-Mashak, E. M., & Tsong, T. Y. (1985) *Biochemistry 24*, 2884–2888.

Endicott, J. A., & Ling, V. (1989) *Annu. Rev. Biochem. 58*, 137–171.

Gill, D. R., Hyde, S., Higgins, C. F., Valverde, M. A., Mintenig, G. M., & Sepúlveda, F. V. (1992) *Cell 71*, 23–32.

Gottesman, M. M., & Pastan, I. (1988) *J. Biol. Chem. 263*, 12163–12166.

Grinstein, S., & Dixon, J. (1989) *Physiol. Rev. 69*, 417–481.

Grinstein, S., Cohen, S., & Rothstein, A. (1984) *J. Gen. Physiol. 83*, 341–369.

Gros, P., Talbot, F., Tang-Wai, D., Bibi, E., & Kaback, H. R. (1992) *Biochemistry 31*, 1992–1998.

Hammond, J. R., Johnstone, R. M., & Gros, P. (1989) *Cancer Res. 49*, 3867–3871.

Hasmann, M., Valet, G. K., Tapiero, H., Trevorrow, K., & Lampidis, T. (1989) *Biochem. Pharmacol. 38*, 305–312.

Higgins, C. F., & Gottesman, M. M. (1992) *Trends Biochem. Sci. 17*, 18–21.

Hope, M. J., Redelmeier, T. E., Wong, K. F., Rodrigueza, W., & Cullis, P. R. (1989) *Biochemistry 28*, 4181–4187.

Iversen, J. G. (1976) *J. Cell Physiol. 89*, 267–276.

Kachel, V. (1990) in *Flow Cytometry and Sorting*, 2nd ed., pp 45–80, Wiley-Liss Inc., New York.

Keizer, H. G., & Joenje, H. (1989) *J. Natl. Cancer Inst. 81*, 706–709.

Kopito, R. R., & Lodish, H. F. (1985) *Nature 316*, 234–238.

Kudrycki, K. E., Newman, P. R., & Schull, G. E. (1990) *J. Biol. Chem. 265*, 462–471.

Laborda, J. (1991) *Nucleic Acids Res. 19*, 3998–3999.

Laris, P. C., & Hoffman, J. F. (1986) in *Optical Methods in Cell Physiology* (DeWeer, P., & Salzberg, B. M., Eds.) pp 199–210, Wiley-Interscience Inc., New York.

Lee, B. S., Gunn, R., & Kopito, R. R. (1991) *J. Biol. Chem. 266*, 11488–11454.

Loew, L., Cohen, L. B., Dix, J., Fluhler, E. N., Montana, V., Salama, G., & Wu, J.-y. (1993) *J. Membr. Biol.* (in press).

Lux, S. E., John, K. M., Kopito, R. R., & Lodish, H. F. (1989) *Proc. Natl. Acad. Sci. U.S.A. 86*, 9089–9093.

Masiakowski, P., Breathnach, R., Bloch, J., Gannon, F., Krust, A., & Chambon, P. (1982) *Nucleic Acids Res. 10*, 7895–7903.

Montana, V., Farkas, D. L., & Loew, L. M. (1989) *Biochemistry 28*, 4536–4539.

Rink, T. J., Montecucco, C., & Tsien, R. Y. (1980) *Biochim. Biophys. Acta 595*, 15–30.

Roepe, P. D. (1992) *Biochemistry 31*, 12555–12564.

Roepe, P. D., Carlson, D., Scott, H., & Wei, L.-Y. (1992) *J. Gen. Physiol. 100*, 52a.

Roos, A., & Boron, W. F. (1981) *Physiol. Rev. 61*, 296–434.

Rottenberg, H. (1979) *Methods Enzymol. 55*, 547–569.

Safa, A. (1988) *Proc. Natl. Acad. Sci. U.S.A. 85*, 7187–7191.

Sambrook, J., Fritsch, E. F., & Maniatis, T. (1989) *Molecular Cloning: A Laboratory Manual*, Cold Spring Harbor Laboratory Press, Cold Spring Harbor, NY.

Sardet, C., Franchi, A., & Pouysségur, J. (1989) *Cell 56*, 271–280.

Savitzky, S., & Golay, G. (1964) *Anal. Chem. 36*, 1627–1639.

Siegfried, J. M., Burke, T. G., & Tritton, T. R. (1985) *Biochem. Pharmacol. 34*, 593–598.

Thiebaut, F., Currier, S. J., Whitaker, J., Haugland, R. P., Gottesman, M. M., Pastan, I., Willingham, M. C. (1990) *J. Histochem. Cytochem. 38*, 685–690.

Valverde, M., Diaz, M., Sepúlveda, F. V., Gill, D. R., Hyde, S. C., & Higgins, C. F. *Nature 355*, 830–833.

Vayuvegula, B., Slater, L., Meador, J., & Gupta, S. (1988) *Cancer Chemother. Pharmacol. 22*, 163–168.